

# Low-frequency passive seismic experiments in Abu Dhabi, United Arab Emirates: implications for hydrocarbon detection

Mohammed Y. Ali<sup>1\*</sup>, Karl A. Berteussen<sup>1</sup>, James Small<sup>2‡</sup> and Braham Barkat<sup>1</sup>

<sup>1</sup>The Petroleum Institute, P.O. Box 2533, Abu Dhabi, United Arab Emirates, and <sup>2</sup>Managing Consultant, Norway

Received July 2009, revision accepted August 2009

## ABSTRACT

Low-frequency passive seismic experiments utilizing arrays of 3-component broadband seismometers were conducted over two sites in the emirate of Abu Dhabi in the United Arab Emirates. The experiments were conducted in the vicinity of a producing oilfield and around a dry exploration well to better understand the characteristics and origins of microtremor signals (1–6 Hz), which had been reported as occurring exclusively above several hydrocarbon reservoirs in the region.

The results of the experiments revealed that a strong correlation exists between the recorded ambient noise and observed meteorological and anthropogenic noises. In the frequency range of 0.15–0.4 Hz, the dominant feature is a double-frequency microseism peak generated by the non-linear interactions of storm induced surface waves in the Arabian Sea. We observed that the double-frequency microseism displays a high variability in spectral amplitude, with the strongest amplitude occurring when Cyclone Gonu was battering the eastern coast of Oman; this noise was present at both sites and so is not a hydrocarbon indicator. Moreover, this study found that very strong microtremor signals in the frequency range of 2–3 Hz were present in all of the locations surveyed, both within and outside of the reservoir boundary and surrounding the dry exploration well. This microtremor signal has no clear correlation with the microseism signals but significant variations in the characteristics of the signals were observed between daytime and nighttime recording periods that clearly correlate with human activity.

High-resolution frequency-wavenumber ( $f$ - $k$ ) spectral analyses were performed on the recorded data to determine apparent velocities and azimuths of the wavefronts for the microseism and microtremor events. The  $f$ - $k$  analyses confirmed that the double-frequency microseism originates from wave activity in the Arabian Sea, while the microtremor events have an azimuth pointing towards the nearest motorways, indicating that they are probably being excited by traffic noise. Results drawn from particle motion studies confirm these observations. The vertical-to-horizontal spectral ratios of the data acquired in both experiments show peaks around 2.5–3 Hz with no dependence on the presence or absence of subsurface hydrocarbons. Therefore, this method should not be used as a direct hydrocarbon indicator in these environments. Furthermore, the analyses provide no direct evidence to indicate that earthquakes are capable of stimulating the hydrocarbon reservoir in a way that could modify the spectral amplitude of the microtremor signal.

---

\*E-mail: mali@pi.ac.ae

‡Formerly at The Petroleum Institute, Abu Dhabi, United Arab Emirates.

## INTRODUCTION

The ambient noise of the Earth is generated by many independent sources that affect the overall frequency band of the natural background wavefield. Frequencies below 1 Hz are largely generated by oceanic and large-scale meteorological events (Longuet-Higgins 1950; Peterson 1993; Webb 2007). At frequencies above 1 Hz, the noise wavefield in urban settings is dominated by cultural sources, particularly traffic, whereas in remote sites wind generated noise is the predominant source (Peterson 1993; Withers *et al.* 1996; Young *et al.* 1996; Wilson *et al.* 2002; McNamara and Buland 2004; Marzorati and Bindi 2006; Bonnefoy-Claudet, Cotton and Bart 2006b). Cultural noise typically exhibits daily and weekly cyclical variations linked to human activities (Yamanaka, Dravinski and Kagami 1993; Bonnefoy-Claudet *et al.* 2006b).

The measurement of ambient noise in the frequency band below 1 Hz can help in our understanding of the interaction between the solid earth, oceans and the atmosphere (Greve-meyer, Herber and Essen 2000; Kedar and Webb 2005). Ambient noise in the 1–10 Hz frequency range (commonly known as microtremor) can provide a low-cost and non-invasive exploration solution in urban sites where geotechnical information is often difficult to obtain. As a result microtremor measurements have been used in many studies to determine fundamental resonant frequencies, shear-wave velocities and thicknesses of unconsolidated shallow sediments (Ohuri, Nobata and Wakamatsu 2002; Hartzell *et al.* 2003; Scherbaum, Hinzen and Ohrnberger 2003; Chavez-Garcia and Luzon 2005; Kind, Faeh and Giardini 2005; Picozzi, Parolai and Richwalski 2005; Maresca, Galluzzo and Del Pezzo 2006; Cho, Tada and Shinozaki 2006; Bonnefoy-Claudet *et al.* 2006a; Tada, Cho and Shinozaki 2006, 2007; Chavez-Garcia and Rodriguez 2007; Dutta *et al.* 2007; Wathelet *et al.* 2008; Stephenson *et al.* 2009). These data can be used to predict local amplification of ground motion during earthquakes and for the preparation of seismic microzonation maps (Gaull, Kagami and Taniguchi 1995; Ansal, Iyisan and Gullu 2001; Tuladhar *et al.* 2004; Bhattarai 2005). Such information is crucial for seismic hazard assessment. Predictions based on microtremor data have been verified using other seismic techniques. For example, patterns of ground motion amplification observed during earthquakes are comparable to amplification patterns modelled from microtremor data (Horike, Zhao and Kawase 2001; Rodriguez and Midorikawa 2003; Cara *et al.* 2008; Haghshenas 2008). Similarly shallow shear-wave velocities determined from the analyses of microtremor data have been verified through ap-

plication of downhole measurements and seismic refraction profiles (Liu *et al.* 2000; Louie 2001; Di Giulio *et al.* 2006).

In addition, microtremor data have been used to image subsurface sedimentary structures. Draganov *et al.* (2007, 2009) used seismic interferometry to cross-correlate ten hours of microtremor data acquired in desert areas of Saudi Arabia and Northern Africa. The cross-correlation revealed several P-wave reflection events that correlated well with reflections deduced from an active seismic survey at the same locations.

In more recent times it has been suggested that microtremor measurements can be used to determine the location, depth and thickness of hydrocarbon reservoirs. Anomalously high spectral amplitudes of microtremor signals in the 1–6 Hz frequency range, with a peak around 3 Hz, have been observed and reported over a number of hydrocarbon reservoirs, primarily in a gas field in Austria and several sites in the Middle East, including some oilfields in Abu Dhabi (Singer *et al.* 2002; Dangel *et al.* 2003; Holzner *et al.* 2005a,b, 2006a,b,c, 2007a,b; Frehner *et al.* 2006, 2007; Rached 2006, 2009; Lambert *et al.* 2007, 2009a,b; Steiner, Saenger and Schmalholz 2007; 2008a; Saenger *et al.* 2007b, 2009a; van Mastrigt and Al-Dulaijan 2008; Nguyen *et al.* 2008, 2009; Goertz *et al.* 2009; Saenger, Torres and Artman 2009c). These studies have claimed that a strong correlation exists between microtremor spectral anomalies and the presence of hydrocarbons over several established oilfields. Their findings suggest that microtremor anomalies diminish towards the rim of hydrocarbon reservoirs and are totally absent above non-reservoir locations.

Furthermore, it has also been suggested that microtremor analysis has several potential applications in hydrocarbon exploration and production. These include reconnaissance of frontier exploration areas, optimization of well placement, reservoir monitoring and as a complementary tool to structural imaging to reduce drilling risk (Holzner *et al.* 2005c; Schmalholz *et al.* 2006; Bloch and Akrawi 2006; Graf *et al.* 2007; Saenger *et al.* 2007a, 2009b). Some studies have suggested that a linear relationship can be derived between the observed microtremor signal and the total thickness of hydrocarbon-bearing layers from various oilfields, mainly in the Middle East (Dangel *et al.* 2003; Holzner *et al.* 2005c; Bloch and Akrawi 2006; Saenger *et al.* 2007a). Other studies have claimed that these anomalous microtremor signals are produced from resonant scattering and amplification within the porous multi-phase (or partially-saturated) reservoir rocks (Holzner *et al.* 2005c, 2009; Schmalholz *et al.* 2006; Graf *et al.* 2007; Saenger *et al.* 2007a, 2009a,b; Walker 2008; Frehner, Schmalholz and Podladchikov 2009). In these theories, it is

assumed that the low-frequency ambient noise (microseisms) of the Earth is the stimulus for the anomalous microtremor signals observed. These studies also claimed that non-linear interaction of the microseism signal with liquid hydrocarbons, water and the pore-rock materials in the reservoirs distorts the ambient noise, resulting in the anomalously high vertical-component microtremor ground velocities above hydrocarbon reservoirs. To date there has not been any published work that successfully applies modelling or mathematical expressions to link microtremor signals with subsurface hydrocarbon reservoirs.

Steiner, Saenger and Schmalholz (2008b) applied time reverse modelling to argue that microtremor data can accurately determine locations, depths and thicknesses of hydrocarbon reservoirs. However, it has since been noted that the time reverse modelling presented in that study was largely controlled by the *a priori* velocity model and was minimally affected by the microtremor wavefield (Green and Greenhalgh 2009).

Furthermore, a growing number of case studies have cast doubt upon the applicability of the microtremor technique for hydrocarbon detection. Berteussen (2008a,b) and Ali *et al.* (2007, 2009a,b,c,d) showed that the observed anomalous microtremor signals are not related to body waves originating from hydrocarbon reservoirs. Rather, they are caused by low apparent velocity surface waves travelling through shallow sediments. In another study, Hanssen and Bussat (2008) analysed ambient noise recorded over an oilfield in the Sahara desert of Libya and suggested that high spectral amplitude microtremor noise does not originate from the underlying reservoir but rather are surface waves caused mainly by anthropogenic noises.

In this paper we present the results of microtremor investigations carried out over an onshore carbonate oilfield and around a dry exploration well in Abu Dhabi, United Arab Emirates. The aims of the experiments were to determine the characteristics and origin of microtremor signals and to investigate whether microtremor signals can be used as a hydrocarbon indicator. We performed frequency, joint time-frequency, V/H (vertical-to-horizontal) spectral ratio, frequency-wavenumber and particle motion analyses to characterize the recorded ambient noise.

## SURVEY AREAS

### Geological setting

#### *Oilfield*

The oilfield for the study is located onshore in the Abu Dhabi Emirate, about 50 km southwest of Abu Dhabi city (Fig. 1a,b).

The field has a moderate relief anticlinal structure and is limited by three major faults, two NW-SE trending and a WNW-ESE trending fault system. The anticline is interpreted to have resulted from vertical movements due to basement tectonics and later compressional stress related to regional tectonics associated with the obduction of the Oman ophiolites in the Late Cretaceous. In addition, the field is affected by the collision of the Arabian Plate with central Iran along the Zagros suture, together with the culmination of the Musandam peninsula during Oligocene-Miocene times. This resulted in deformations related to strike-slip movements. However, the main phase of deformation occurred during the Late Cretaceous. The shallow subsurface structure of the field consists mainly of soft Quaternary sediments overlying hard Tertiary carbonates.

The producing zones are all within a series of stacked reservoirs of the Lower Cretaceous Shuaiba and Kharaib Formations, all from the Thamama Group (Barremien to Late Aptian) (Fig. 2). These carbonate reservoir intervals are separated by very low porosity intervals that are commonly referred to as dense zones. The reservoir zones correspond to the late transgressive and highstand system tracts characterized by parasequence sets that show shoaling upward trends of predominantly aggradational and progradational stacking patterns.

The vertical closure at the main reservoir level is approximately 40 m. This oilfield was selected as a suitable site for the experiment because it has a clear and well-defined oil/water contact (OWC) mapped from 3D seismic and well data according to geoscientists currently working on the field. However, there is a slight possibility that deeper reservoirs (e.g., in the Upper Jurassic Arab and Permian Khuff Formations) may exist in the field. Nevertheless, the oilfield provides a unique environment in which to measure and study the microtremor signal both above and outside the reservoir.

#### *Dry exploration well*

The deep exploration well is located about 100 km southeast of Abu Dhabi city (Fig. 1a,b). The well was drilled with a near-surface geology characterized by tens of metres of poorly-consolidated aeolian Quaternary sediments. The seismic interpretation indicated the presence of small closures at Kharaib Formation level. The well targeted a closure with an elongated structural feature striking in a NW-SE direction encompassing two culminations, being bound from the west by a normal fault dipping to the west. The main exploration objectives of the well were to investigate the hydrocarbon potential and reservoir development of the Mishrif, Shuaiba

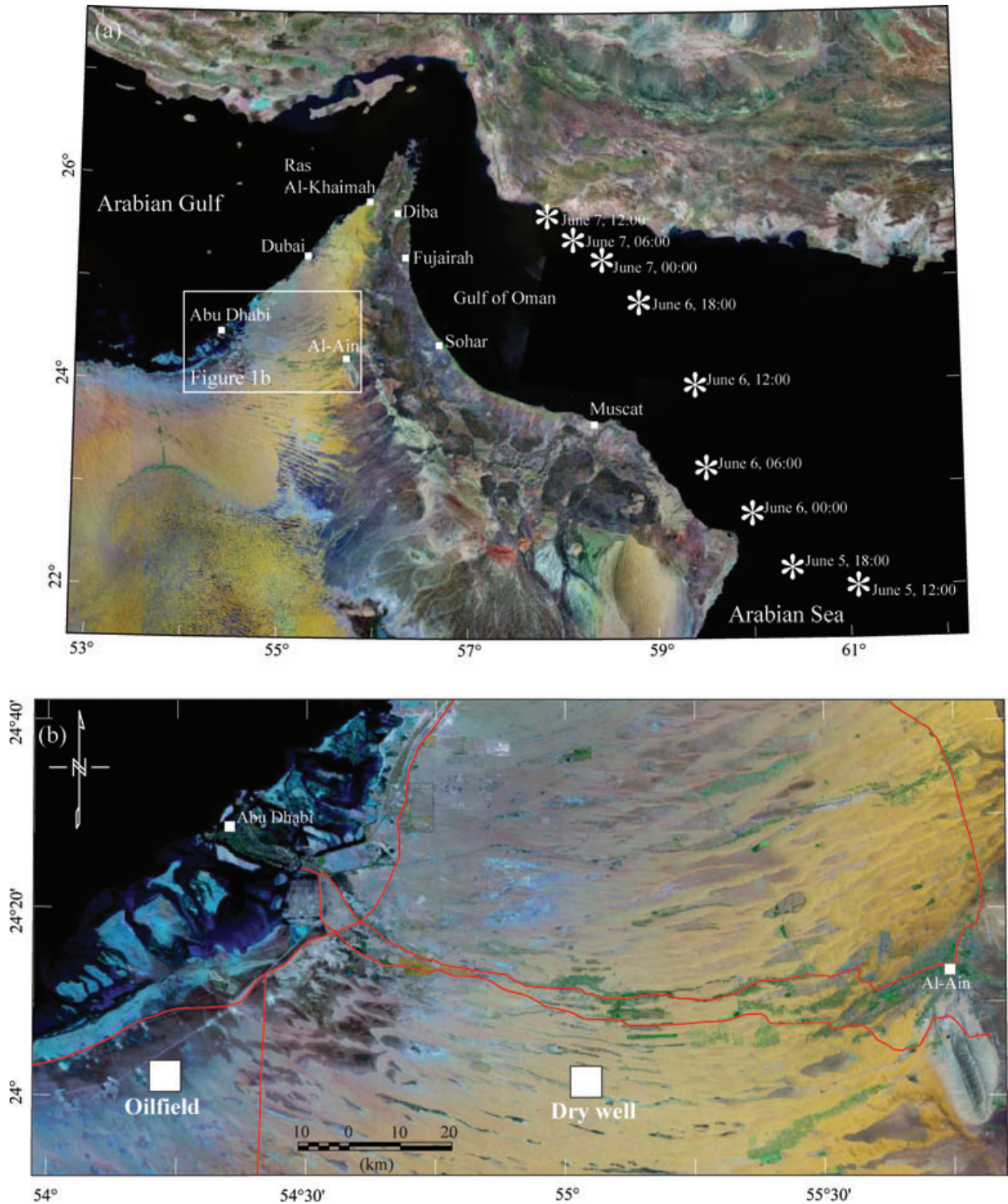


**Figure 1** a) Regional satellite map showing the study areas. Stars show the location and date/time of Cyclone Gonu. b) Local satellite map showing the study areas. Red lines show major motorways. c) Location map of the survey on the oilfield showing the oil/water contact (OWC). Red triangles represent the position of the seismometers above the oil reservoir, whereas blue triangles represent the location of the seismometers above the water saturated zone. d) Location map of the survey on the abandon exploration well. Red triangles indicate the position of the seismometers.

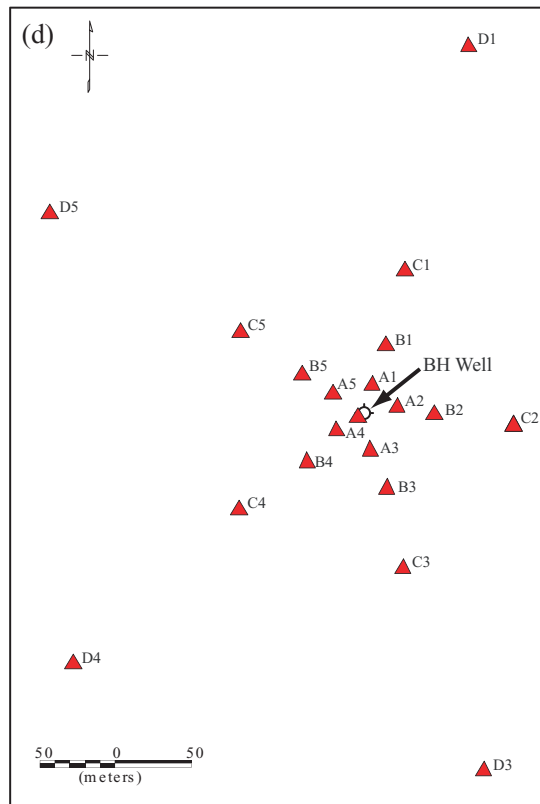
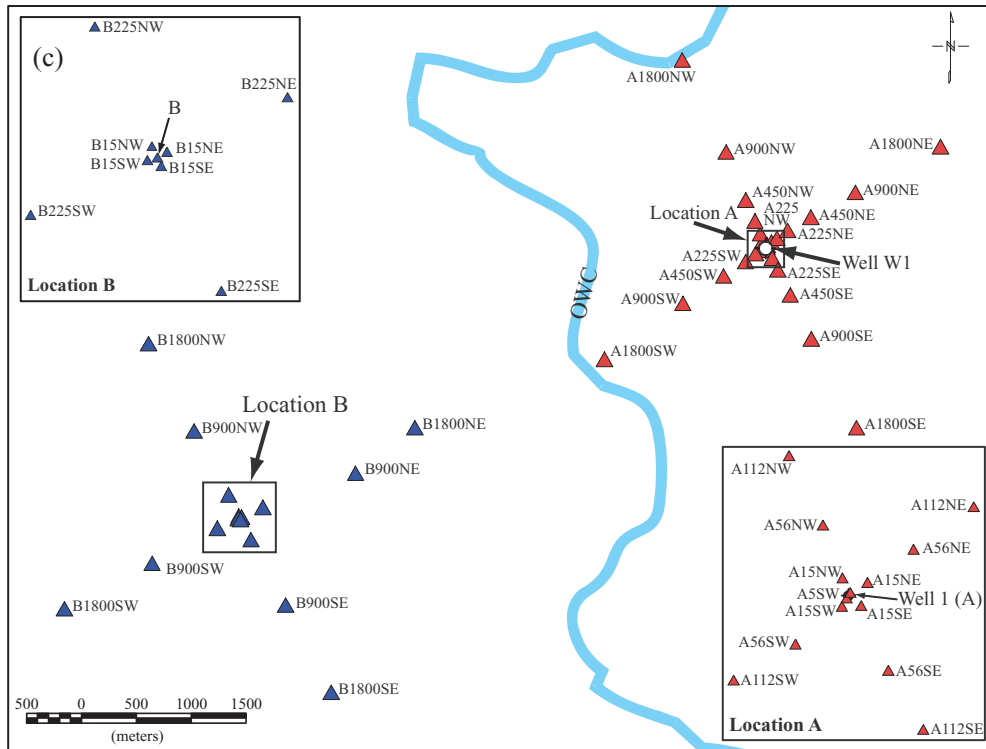


Figure 1 Continued.

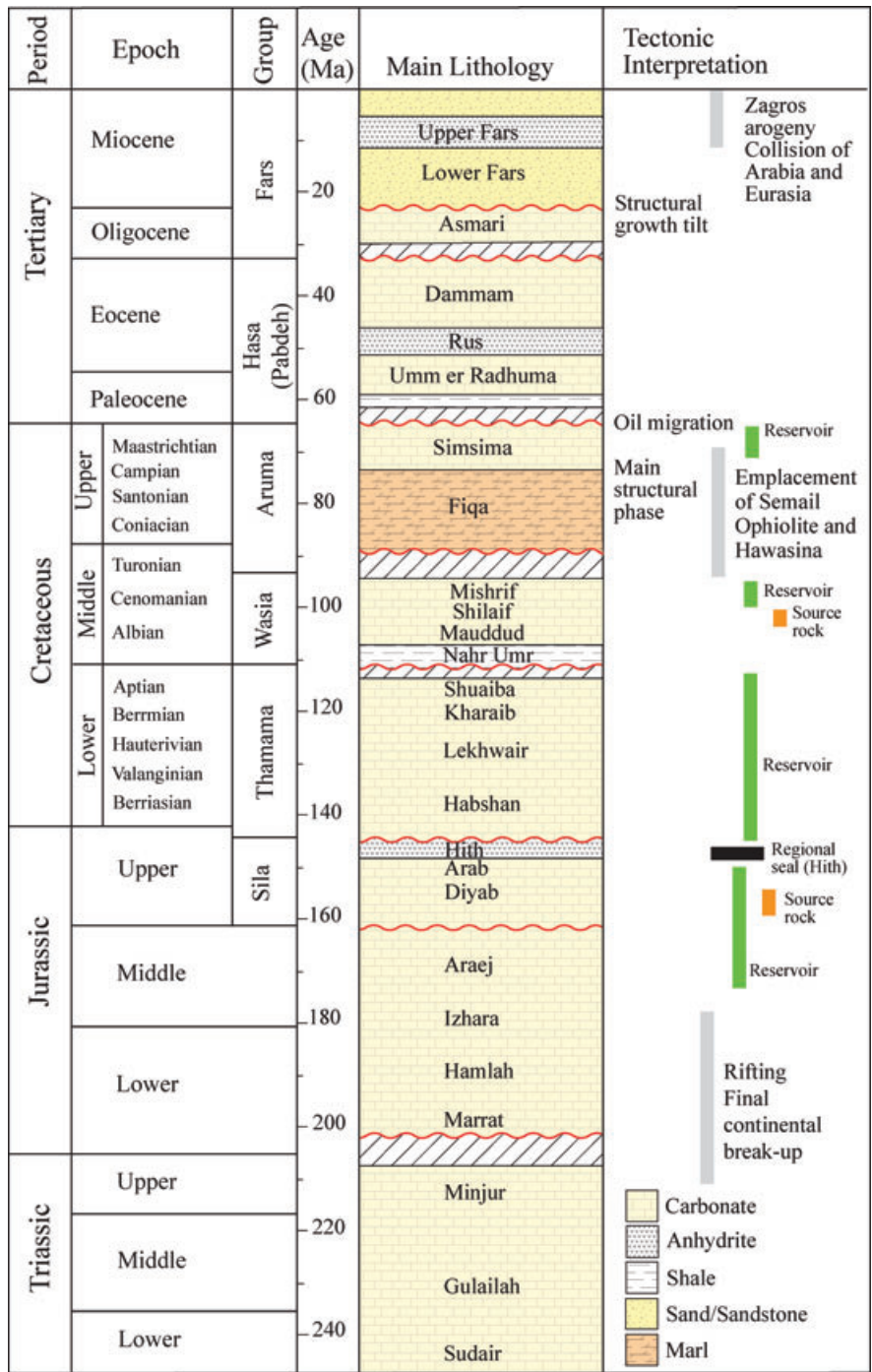


Figure 2 Summary of stratigraphic column of the UAE foreland basin showing petroleum systems of Mesozoic and Tertiary. Modified from Ali and Watts (2009).

(Middle-Lower Cretaceous) and the deeper Upper Jurassic Formations (Fig. 2). The well eventually penetrated more than 16 500 ft of Mesozoic and Cenozoic sediments but logging data indicated that the characteristics of all prospective reser-

voirs were insignificant. Moreover, open hole drillstem tests (DST) and production tests of the reservoirs were all found to be water-bearing. While this area was specifically chosen for the study primarily because of the lack of hydrocarbons

present, there is always the possibility that deeper reservoirs could exist (e.g., in the Khuff Formation). However, the seismic data show no clear structures that could trap significant accumulation of hydrocarbons below the Upper/Middle Jurassic Formations.

### Data acquisition

The survey over the oilfield was carried out between 21 May and 17 June of 2007. During the acquisition of the data, a powerful tropical cyclone (Cyclone Gonu) hit the coast of Oman (Fig. 1a). Cyclone Gonu developed in the eastern Arabian Sea on 1 June attaining peak wind speeds of 240 km/h on 3 June. Cyclone Gonu made landfall on the eastern coast of Oman on 5 June with sustained wind speeds of approximately 150 km/h, becoming the strongest tropical cyclone to hit the Arabian Peninsula in recorded times (De Bhowmick *et al.* 2007; le Comte 2008). It then turned northward into the Gulf of Oman and dispersed after moving ashore along southern Iran on 7 June.

The survey consisted of a single 2D profile running between locations A and B, with several detailed studies conducted around each of these locations using arrays of sensors (Fig. 1c). The array geometry was designed to optimize the detection of microseism and microtremor signals. Location A is situated over the maximum oil column of the reservoir, whereas location B was positioned over an area that presumably contained no oil. The 2D seismic profile was recorded simultaneously and intended to connect the two sites. Two seismometers were placed at locations A and B to continuously record throughout the entire survey and to monitor any long-term variations in the ambient noise. The deployment of the sensor arrays consisted of 7 individual configurations centred at location A and 4 configurations at location B, each with varying aperture sizes (from 30–3600 m). Each array consisted of 5 broadband stations and utilized a typical recording period of 24 hours.

The survey over the dry exploration well was carried out in January of 2009 and included the deployment of four arrays with varying aperture sizes (50–500 m) centred at the well (Fig. 1d). Recording times for the arrays varied from 1–24 hours.

The signals were recorded using 3-component broadband seismometers, Guralp CMG-6TD for the first experiment over the oilfield and CMG-3EX for the second experiment around the dry exploration well. Each sensor was equipped with an internal 24-bit digitizer and external global positioning system (GPS) receiver to allow precise synchronization of the mea-

surements. The seismometers have a flat frequency response from 0.33–100 Hz, with a sensitivity of 2000 V/m/s. A sampling rate of 200 Hz was used for the first experiment and 100 Hz for the second experiment. The sensors were covered and buried up to 0.5 m deep where possible for firm ground contact and wind shielding.

### Data processing

Time, frequency and joint time-frequency analyses were performed to characterize the recorded ambient noise. Data were first converted into units of metres per second by correcting for the digitizer output and the seismometer gain factor. A processing window of 60 seconds with a 5% cosine taper was applied to the data to reduce spectral leakage. Fourier amplitude spectra were analysed, both without smoothing applied and with the smoothing procedure of Konno and Ohmachi (1998), using a *b*-value of 40. The mean was removed and excessively noisy sections of the signal were excluded from the analyses before stacking the data. Figure 3 shows that strong local wind conditions and regional earthquakes can contaminate the signal by generating high-frequency (>6Hz) and low-frequency (<2 Hz) noises respectively. Such noisy data were removed prior to analyses.

Time-frequency representations were used to analyse the spectral content of the data. Time-frequency representations have been successfully used for signal recovery at low signal-to-noise ratio, for accurate estimation of the instantaneous frequency, for signal detection in communication, for radar and for the design of time-varying filters (Cohen 1995). The time-frequency representation technique that was used in this study is the short-time Fourier transform, defined as

$$X(t, f) = \int_{-\infty}^{\infty} x(\tau)h(\tau - t)e^{-j2\pi f\tau} d\tau \quad (1)$$

where  $x(\tau)$  is the signal under investigation and  $h(t)$  is a window function centred around  $t = 0$ . The Fourier transform is generated by shifting the window so that it is centred on a time of interest, multiplying  $x(\tau)$  by the shifted version of  $h(t)$  and then taking the Fourier transform of the resultant windowed signal. The window can be shifted such that the resulting time intervals are contiguous or overlapping. In the examples below (Figs 6 and 10), contiguous windows were considered.

### ANALYSIS OF AMBIENT NOISE

Continuous recording over a period of 27 days allowed the time response of the ambient seismic noise to be correlated with large-scale meteorological conditions and anthropogenic

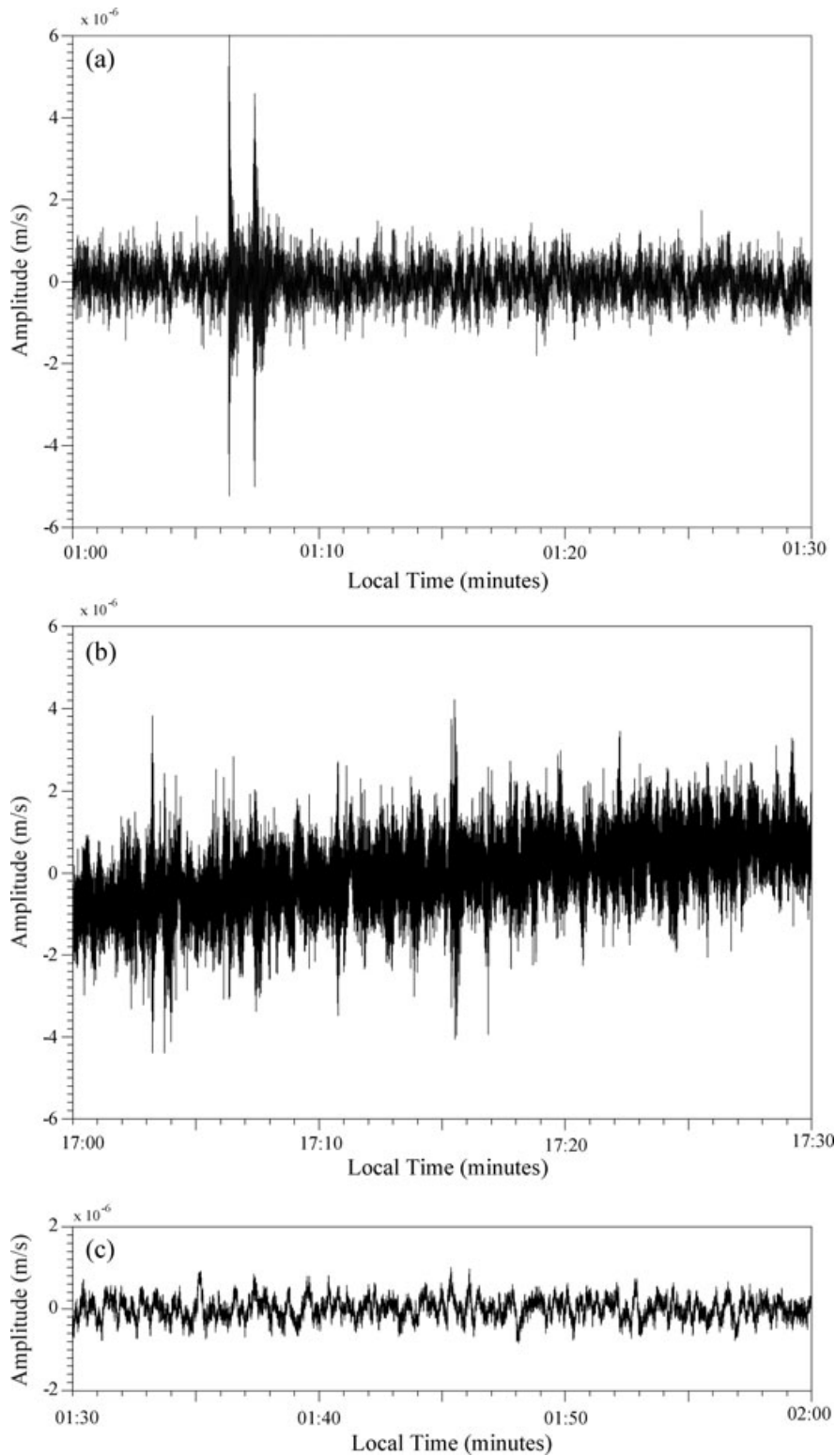


**Figure 3** Time series of vertical particle velocity showing a) a regional earthquake that occurred in southern Iran on early morning (local time) of 8 July 2007. b) A noisy data set probably due to windy conditions. c) Quiet data set. d) Spectral amplitudes of the records displayed in Fig. 3(a–c).

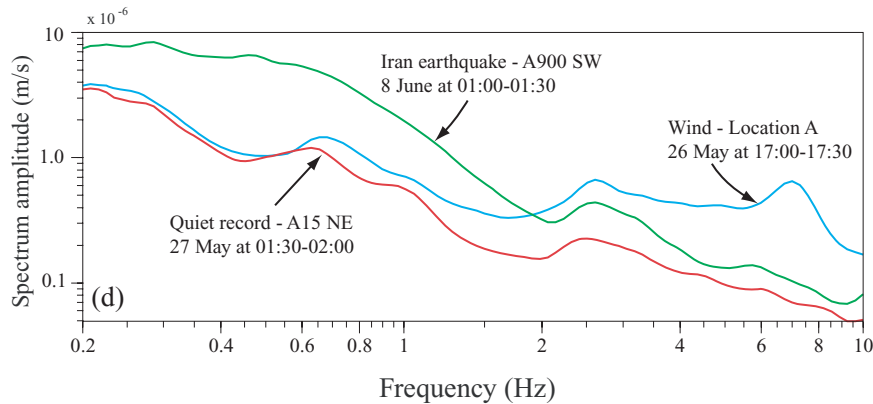


Figure 3 Continued.

noises. Figure 4 shows the ambient noise observed at the two sites. Many of the features of the figure are well understood and include microseism (0.1–1 Hz) and microtremor (2–6 Hz) signals. In this section the noise spectra amplitude estimated for the two survey areas in these bands are detailed.

#### Frequencies below 1 Hz

Figure 4(a–c) shows representative spectral amplitudes of the ambient noise recorded at locations A and B of the oilfield and close to the dry exploration well, respectively. In the frequency range 0.15–0.4 Hz, the noise spectrum is dominated by a strong and easily recognizable peak at 0.25 Hz called the double-frequency peak (Longuet-Higgins 1950). The peak of the double-frequency microseism spectrum occurs at a frequency nearly twice that of the ocean surface waves (Longuet-Higgins 1950; Bromirski and Duennebieer 2002). It is believed that this double-frequency microseism occurs as a result of the non-linear interaction between two ocean swells with the same frequency, propagating in opposite directions (Longuet-Higgins 1950; Friedrich, Krüger and Klinge 1998; Kedar and Webb 2005; Tanimoto 2007; Webb 2007). The conditions that generate a double-frequency microseism arise in shallow water due to the interaction of incident ocean swells and reflected/scattered wave energy from coastal areas (Bromirski and Duennebieer 2002; Bromirski, Duennebieer and Stephen 2005). This noise occurs at all sites and thus can not be correlated with the presence of hydrocarbons.

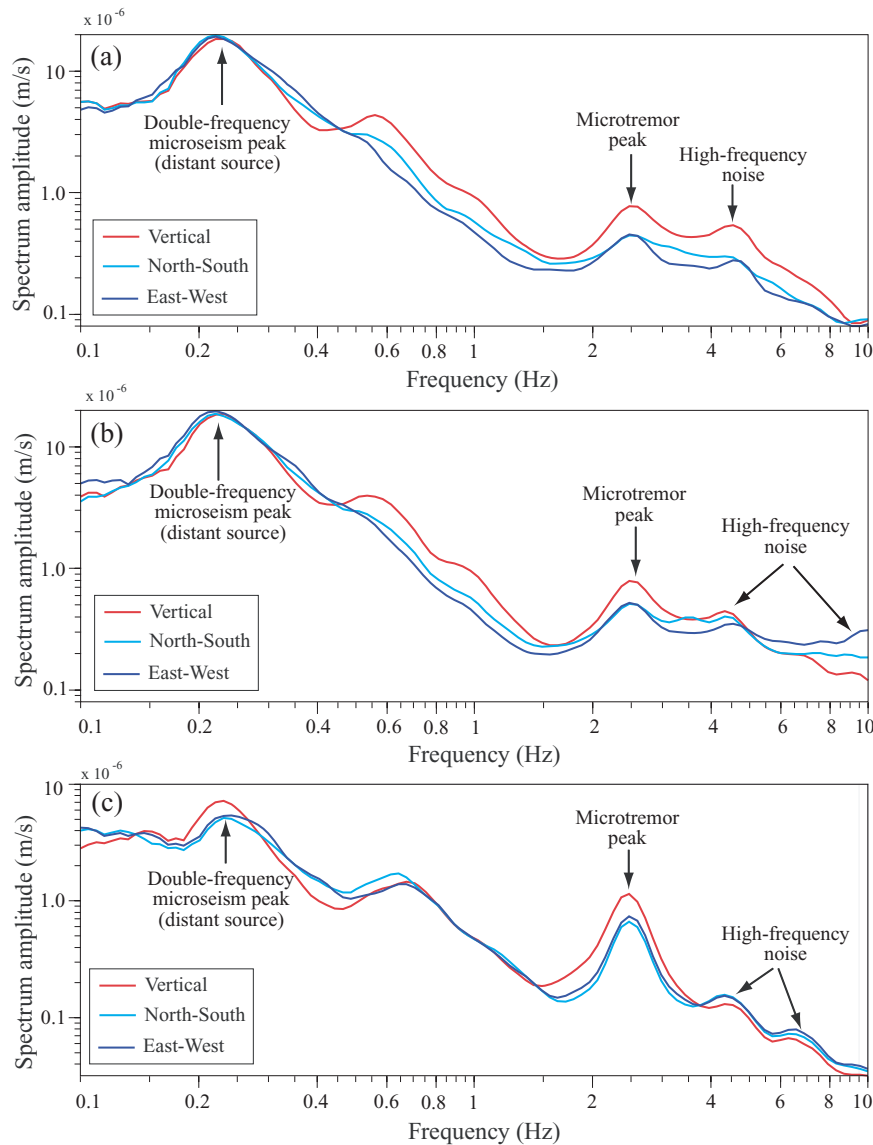
#### Frequencies above 1 Hz

Figure 5(a) shows the spectral amplitude of the 2D profile running from location A to location B of the survey over the oilfield. The figure shows a distinct spectral microtremor anomaly that peaks at about 2.5 Hz. The microtremor signal is observed on all stations whether positioned over the

oil reservoir (location A) or over the water saturated zone (location B), with no significant differences in the spectral amplitudes of microtremors signal inside or outside the reservoir boundary. In addition, all three components (vertical, north-south and east-west) for all stations recorded the signal (Fig. 4). This observation is confirmed by the second experiment over the dry exploration well, which shows a distinct microtremor signal at about 2.5 Hz on all three components (Fig. 5b). The figure shows that the spectral amplitude of microtremors at the dry well are much higher than that of the oilfield.

The spectral amplitude of microtremor signals recorded in these surveys exhibited distinctive cyclical day-to-night and weekdays-to-weekend variations. During the daytime a strong microtremor signal consistently appears, whereas during the night only weak microtremor signals were detected (Fig. 6a,b). The 24-hour cycle has minimum amplitude at around 1 am local time and maximum amplitude late in the morning. In addition, low microtremor amplitudes were observed during the weekend (Fridays in the United Arab Emirates) compared with a typical weekday. In the dry well location, differences of spectral amplitude of the microtremor signal were observed between daytime and nighttime measurements. In contrast, the microseism signal shows negligible day and night variation, suggesting that the source of the signal is not dependant on the local anthropogenic activity.

These microtremor signals have been attributed to the non-linear interaction of the microseism signal with the hydrocarbon reservoir, causing enhanced vertically polarized P-waves in the microtremor band above the reservoir compared with positions away from the reservoir (Holzner *et al.* 2005c; Graf *et al.* 2007; Walker 2008; Saenger *et al.* 2009b). However, the fact that all three components have recorded the signal means that the signal cannot possibly be a direct P-wave travelling vertically up from below the sensors, unless it has been



**Figure 4** Examples of typical spectral amplitudes of 60 minute periods of ambient noise recorded on vertical and horizontal components at a) location A of the oilfield survey, 7 June 2007 at 00:00–01:00. b) Location B of the oilfield survey, 7 June 2007 at 00:00–01:00. c) Close to the dry exploration well, 21 January 2009 at 00:00–01:00. All locations show double-frequency microseism at a frequency of around 0.25 Hz, microtremor at around 2.5 Hz and high-frequency noise. Microseism and microtremor signals were observed on all three seismometer components (vertical, north-south and east-west) at all recording stations. For sensor locations see Fig. 1.

scattered or converted. In addition, the strong diurnal variation in the microtremor signal suggests that the source responsible is possibly related to surface waves caused by the coupling of anthropogenic noise (e.g., traffic, production installations), which tend to have minimums at night and on weekends due to the cyclical nature of cultural noise. Such daily and weekly variations in spectral amplitudes of microtremor signals have been reported in many other studies that have attributed cultural activities revealed by regular daily spectral

amplitude variations with minimums recorded at midnight and maximums at midday (Yamanaka *et al.* 1993; Bonnefoy-Claudet *et al.* 2006b).

#### COMPARISON OF AMBIENT NOISE WITH METEOROLOGICAL DATA

The correlation between the double-frequency microseism peak and the presence of ocean storms is supported by the

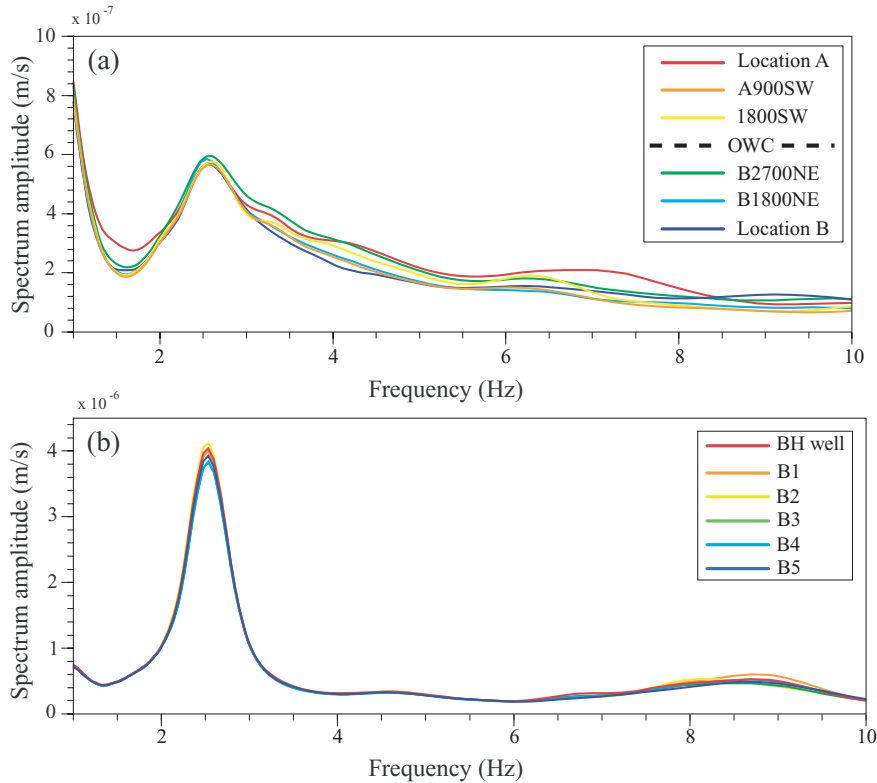


**Figure 5** a) Spectral amplitudes of vertical components of the sensors located along a profile from location A to B on the oilfield on 7 June 2007 at 00:00–01:00. b) Spectral amplitudes of sensors with array aperture of 100 m centred at the exploration dry well on 20 January 2009 at 00:00–01:00. All locations (above and outside the oilfield) show distinct microtremor signal.

temporal variation of spectral levels observed in the first survey during the occurrence of Cyclone Gonu in 2007 (Figs 1a and 7a). Spectral amplitudes of the double-frequency microseism increased as Cyclone Gonu developed then reached their maximum on 6 June as Gonu approached the eastern Omani coast. The spectral amplitudes immediately dropped back again once the cyclone had passed the region. Therefore, the appearance of Cyclone Gonu over the Arabian Sea during 4–6 June effectively explains the larger spectral amplitudes of double-frequency microseisms observed during the survey.

It is not surprising that microseism waves were recorded even at a distance of more than 500 km from the Omani coast. The microseism energy propagates primarily as fundamental Rayleigh waves through the Earth's crust and hence does not attenuate rapidly and may be observed at continental sites far removed from the coastlines (Haubrich and McCamy 1969; Barstow, Sutton and Carter 1989; Bromirski and Duennebieer 2002; Bonnefoy-Claudet *et al.* 2006b). For example, Gerstoft, Fehler and Sabra (2006) reported observ-

ing microseisms in Southern California which were generated by Hurricane Katarina in New Orleans some 2700 km away.

Comparing Fig. 7(a,b) over the duration of the survey indicates there is no direct relationship between the strength of the microtremor and the microseism signals. During the period in which Cyclone Gonu was battering the eastern Omani coast the spectral amplitude level of the microseism signal increased by a factor of about 10. This increase is seen to be essentially identical for both the vertical and horizontal components, whereas the microtremor signal remained seemingly unchanged. Hanssen and Bussat (2008) also noted that there is no correlation between the low-frequency (1–6 Hz) band and microseism signal (<0.25 Hz). This is inconsistent with the assertion made by Holzner *et al.* (2005c, 2009) that the driving force in the generation of the anomalous microtremor signals are microseism events.

Winds can be considered as broadband sources producing large amplitudes of noise at high frequencies (>1 Hz), representing fluctuations in response to the variation of the wind intensity (Withers *et al.* 1996; Young *et al.*

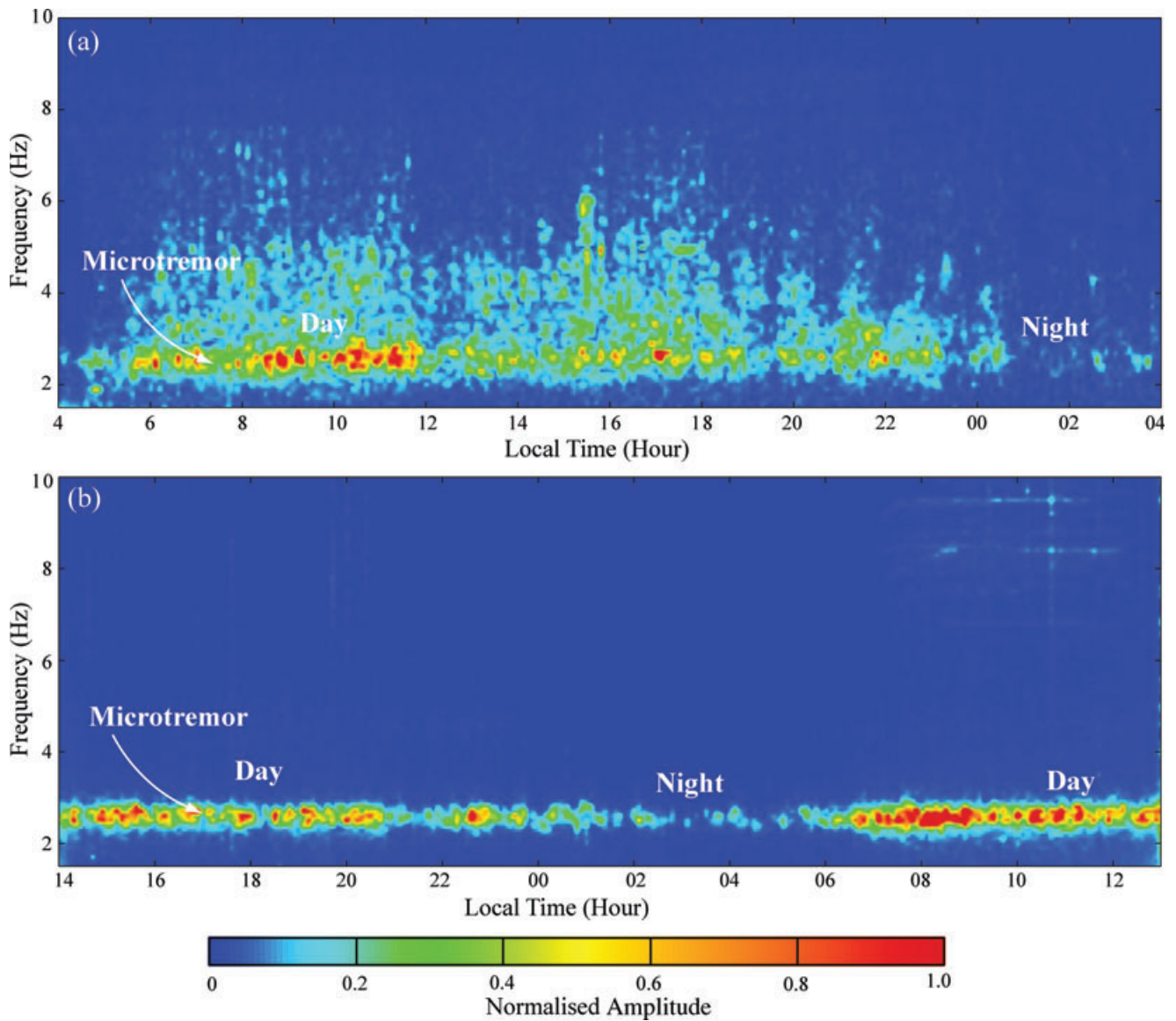


**Figure 6** a) Time frequency display for data recorded from the vertical component of the seismometer at location A of the oilfield on 26 May 2007. b) Time frequency display for data recorded from the vertical component of the seismometer close to the dry exploration well on 20 January 2009. On both locations the microtremor signal exhibits strong diurnal variations with a strong signal during the day and a weaker signal at night.

1996). Hence, we compared the microtremor measurements with local wind speed and temperature obtained from a weather station located approximately 30 km north-east of the oilfield.

Figure 8(a-c) shows a comparison of microtremor signals recorded on the oilfield with meteorological data (wind speed and temperature). The figure shows that the maximum spectral amplitude of microtremor signal occurs at about 8:00 am local time, which corresponds to the period with lowest av-

erage wind speed (2–3 km/s) and relatively low temperature (33° C). The highest temperature (>45° C), which occurs at around midday, correlates well with a period of relatively low microtremor spectral amplitude, which is probably due to there being less cultural noise at that time (lunch and prayer breaks). The lack of a direct correlation between the fluctuations in spectral amplitudes of the microtremor and wind speed is probably due to the isolating effects of burying the seismometers to a depth of 0.5 m. However the separation

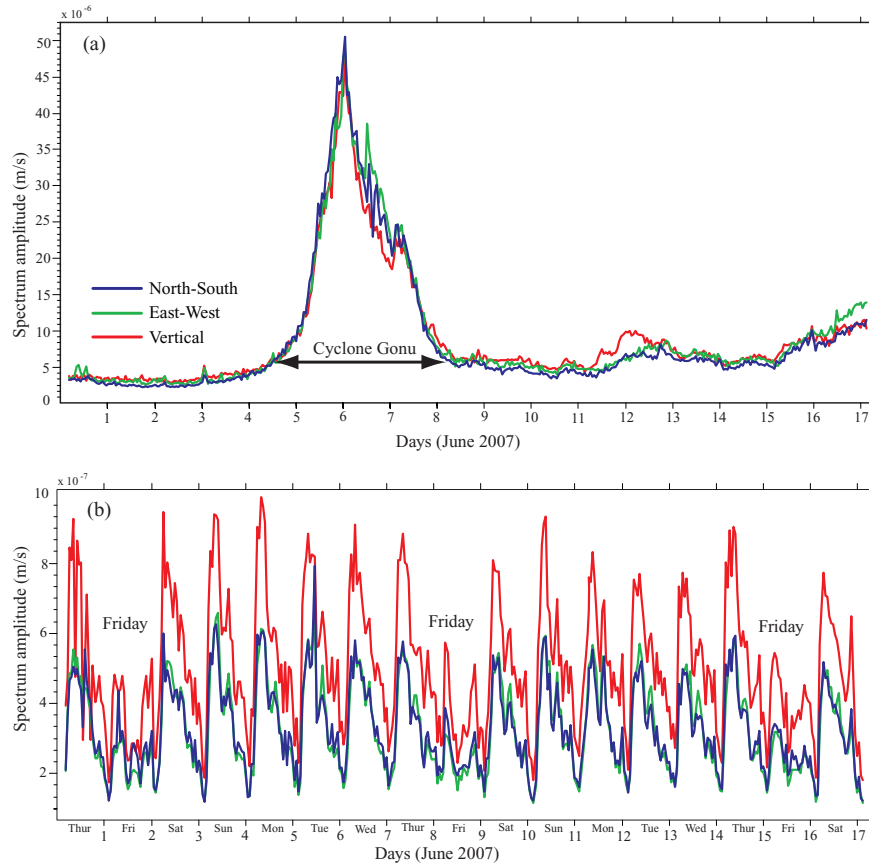


**Figure 7** a) Peak spectral amplitude of horizontal and vertical components of double-frequency microseism (about 0.25 Hz) obtained at location B of the oilfield. b) Peak spectral amplitude of microtremor signal (2.5 Hz) horizontal and vertical components recorded at location B of the oilfield. The spectral amplitudes of microseisms increased dramatically when Cyclone Gonu approached the coast of Oman, whereas the microtremor signal remained unchanged. Spectral amplitudes of microtremor signals exhibit strong daily and weekly cyclical variations. Signals were significantly stronger during normal working hours on weekdays compared with nighttimes and across weekends (Fridays in the United Arab Emirates).

(30 km) between the weather station and the survey may also affect this.

### VERTICAL/HORIZONTAL SPECTRAL RATIOS

The H/V spectral ratio technique (Nakamura 1989) consists of estimating the ratio between the Fourier amplitude spectra of the horizontal and the vertical components of the microtremor recorded at the ground surface. The method takes advantage of the fact that, in a soft soil layer, horizontal ground movements (mainly Rayleigh waves) are more strongly amplified than the vertical movements. As a result, there is a correlation between the H/V peak frequency and the fundamental resonance frequency of the site. The technique provides reliable estimates of fundamental resonance frequency and am-

plification factors of the uppermost soft layers (Nakamura 1989; Lermo and Chavez-Garcia 1994; Konno and Ohmachi 1998).

It has been suggested that the dominant amplitude peak of the ratio of vertical to horizontal components (V/H) in the microtremor range is higher over hydrocarbon reservoirs (Lambert *et al.* 2007). The proponents of this assertion reason that hydrocarbon reservoirs emit distinctive P-waves that cause an increased vertical polarization of the ambient noise wavefield at the surface. This suggestion has resulted in the premise that high V/H values ( $>1$ ) can be used as a direct hydrocarbon indicator (Walker 2008; Lambert *et al.* 2009a,b; Saenger *et al.* 2009b; Goertz *et al.* 2009; Nguyen *et al.* 2009).

For each station in this study, the spectral amplitudes for the horizontal and vertical components were calculated over

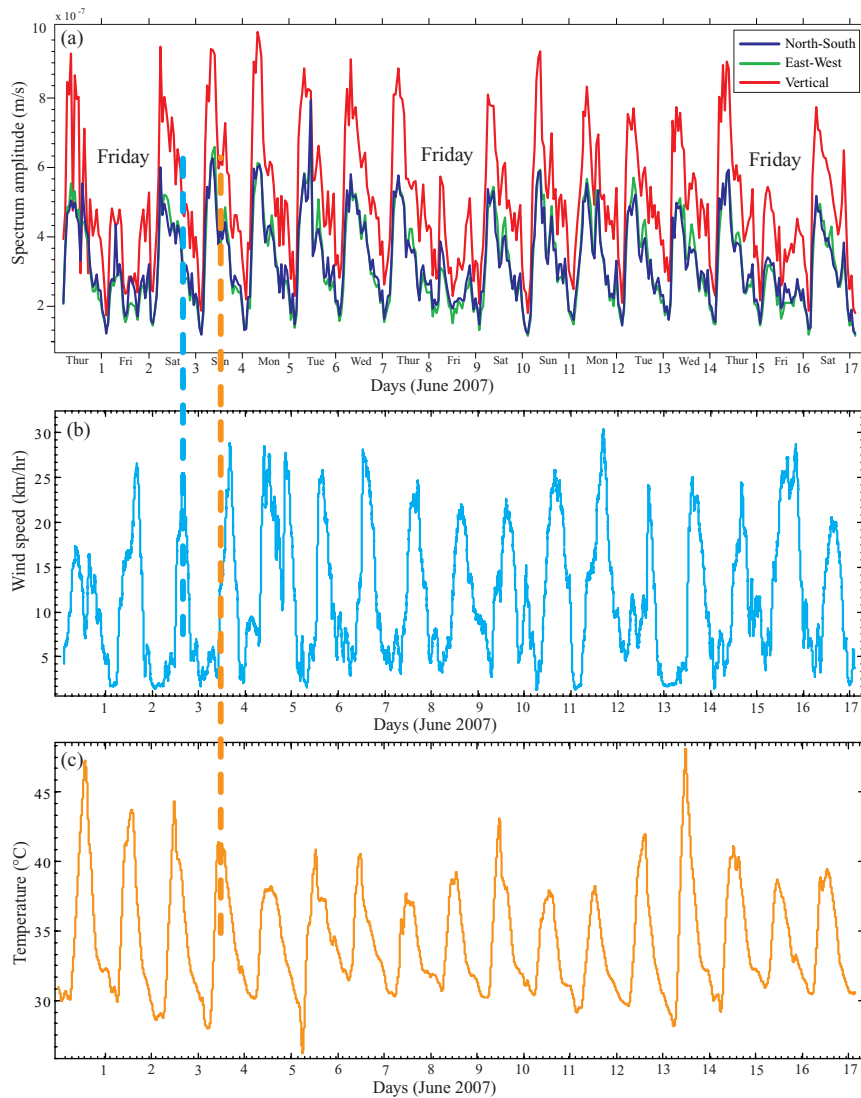


**Figure 8** Comparison of a) peak spectral amplitude of microtremor signal with b) wind speed and c) temperature. Maximum spectral amplitude of microtremor occurs at around 08:00 am local time, which is close to when the wind speed is slowest. Highest temperature at midday correlates well with relatively low spectral amplitude, which is probably due to lunch and prayer break.

a continuous 60-minute period of ambient noise. The Fourier amplitude spectra were then smoothed, following the method of Konno and Ohmachi (1998) and the quadratic mean of the horizontal amplitude spectrum was divided by the corresponding vertical spectrum. The final result was obtained by averaging the H/V ratios from all windows and then inverting to obtain the V/H ratio.

The V/H spectral ratios measured over the oilfield (Fig. 9) indicate that a peak ( $>1$ ) exists at 2–3 Hz on most of the stations whether measured over oil-saturated or water-bearing areas. The anomalous V/H curve obtained at location A, for frequencies higher than 3 Hz, is probably related to localized

noise generated by the structures immediately surrounding well A. The results from V/H analysis for the second experiment over the dry well show an identical V/H peak also at about 2.5 Hz. Hence, these results would indicate that the V/H method could not be used as a hydrocarbon indicator in this case.

## EARTHQUAKE TRIGGERED MODIFICATION

It has been suggested that hydrocarbon reservoirs can be stimulated by earthquake activity to temporarily alter the local

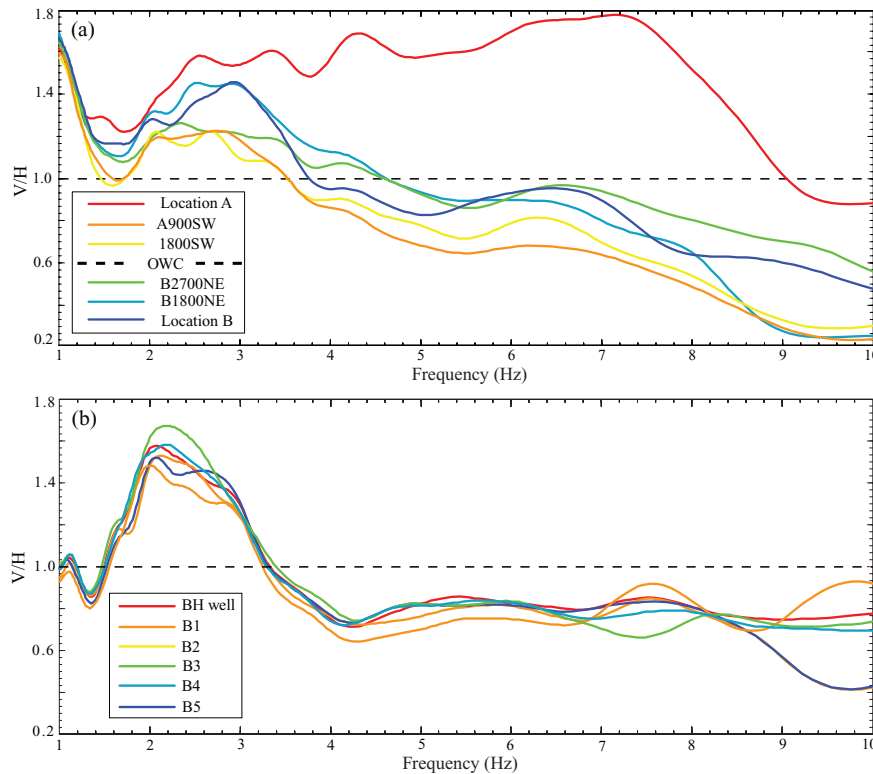


**Figure 9** a) Mean V/H spectral ratio of microtremor data recorded at the oilfield for 60 minutes on 7 June 2007 at 00:00–01:00. b) Mean V/H spectral ratio of microtremor measurement at the dry well for 60 minutes on 20 January 2009 at 00:00–01:00. V/H spectral ratios of 2.5–3 Hz are observed on both sites. The V/H peaks of 2.5–3.0 Hz are observed on both sites. The peaks are not related to the location of the hydrocarbon reservoir.

ambient noise wavefield (Nguyen *et al.* 2008). This stimulation is said to result in a significant spectral increase of the microtremor signal above the reservoir both during the earthquake and for at least an hour after the event. To test this observation, teleseismic and regional earthquakes that were recorded during the survey over the oilfield were examined. An earthquake that occurred in southern Iran on 8 June (local time) with magnitude of 4.2, for example, is shown in Figs 3(a) and 10. The onset of this event is apparent with a sharp increase in the amplitudes of all three components over a wide frequency band. However, there is no clear indication as to whether the spectral amplitude of the microtremor signal is amplified during or after the earthquake. Both the vertical and north-south components actually indicate a slight decrease of spectral amplitude for the microtremor frequencies immediately after the earthquake, which is inconsistent with observations reported by Nguyen *et al.* (2008).

## FREQUENCY-WAVENUMBER ANALYSIS AND WAVE PROPAGATION ACROSS THE ARRAYS

Frequency-wavenumber analyses of array data provide an excellent means for discriminating the seismic wavefield by phase velocity, propagation azimuth and frequency. These in turn provide detailed information on the source generation and propagation modes of noise wavefield (Capon 1969; Haubrich and McCamy 1969; Cessaro 1994; Satoh, Kawase and Matsushima 2001; Okada 2003; Chevrot *et al.* 2007). In this study, we applied high-resolution frequency-wavenumber ( $f-k$ ) spectral analysis to the array data, as proposed by Capon (1969). In doing so, we were able to identify the directions of approach and dominant phase velocities of the microseism and microtremor waves as they moved over the array, thereby distinguishing body waves from surface waves and possibly identifying their origins. The method assumes plane waveform

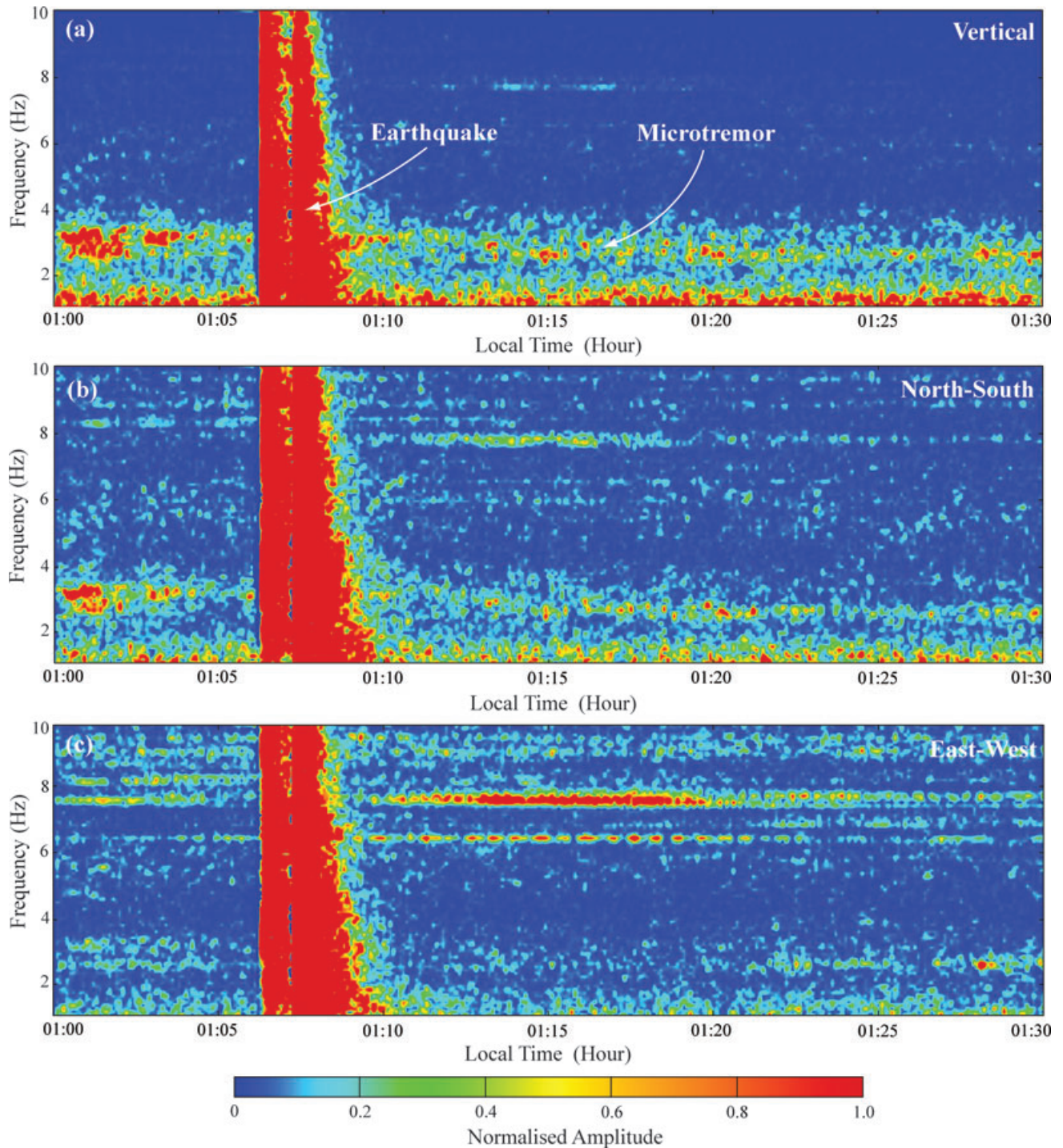


**Figure 10** Time frequency display for data recorded from a) vertical component and b) north-south component. c) East-west component showing that a regional earthquake occurred in southern Iran on early morning (local time) of 8 June 2007 with magnitude of 4.2. The earthquake has a well-defined signature characterized by a vertical streak of high energy over a wide frequency band.

propagation through the seismic array and aims to improve the resolution in wavenumber space.

In this study the propagation azimuth and slowness of the microseism and microtremor bands were measured in each array by finding the peak power in slowness space of continuous 60-minute signal samples. The wavenumber domain was computed on a uniformly sampled grid in  $f$ - $k$  space using vertical component signals from the array recordings.

Figure 11(a,b) shows the slowness maps for microseism bands (centre frequency of 0.25 Hz) in the oilfield from cross-shaped arrays with apertures of 3600 m at locations A and B respectively. While such a cross-shaped array does not have an isotropic mapping pattern, this does not dramatically affect the detection of the azimuth of the approaching wavefield. A straight arrow denotes the corresponding propagation back azimuth for the wavenumber vector at the peak spectrum amplitude. The signal across both arrays exhibits high coherency, showing a single well-defined peak at slowness corresponding to that of crustal Rayleigh waves with apparent velocity of approximately 3600 m/s. This high apparent velocity indicates that the wavefield has interacted with deeper more compacted carbonate rocks, consistent with these low frequencies. The propagation back azimuth (i.e., direction from the array pointing back towards the source) of the wavefront varies from 305–327°, with the slight difference on propagation azimuth most likely due to change in source positions. The wavefront is interpreted as being microseismic events generated by wave activity in the Arabian Sea, far to the south-east.

Figure 11(c) illustrates the slowness map for the microtremor (centre frequency of 2.5 Hz) signal recorded at the oilfield, with array aperture of 225 m. The propagation azimuth is relatively scattered although the maximum energy response is about 180° pointing in the direction away from a major motorway (Fig. 1b). The apparent velocity of the wavefronts is about 1150 m/s. Figure 11(d) illustrates the slowness map for microtremor (centre frequency of 2.5 Hz) measurement recorded at the dry well with array aperture of 200 m. Examination of the phase velocities of the wavefront indicates a tendency to cluster at approximately 800 m/s with a propagation azimuth of 165°, again pointing to the nearest motorway (Fig. 1b).

The study area is composed of shallow unconsolidated sediments, which lie directly over hard carbonate layers with P-wave velocities far above 1150 m/s. Therefore, it is unlikely that the observed wavefront is an ordinary P-wave originating from the subsurface hydrocarbon reservoir. If the recorded waves were actually coming directly from below the array,

then they should arrive simultaneously at all seismometers (i.e., the apparent velocity would be infinite and the azimuth undefined).

On the basis of these observations, the origin of the anomalous microtremor events is interpreted as comprising surface-coupled waves excited mainly by traffic noise from motorways that cross the survey areas at a distance of about 10–15 km (Fig. 1b). This analysis correlates with the interpretation drawn from the spectral amplitude analyses but contrasts with other studies that have attributed the spectral peaks of the microtremor events with the location of subsurface hydrocarbon reservoirs (Dangel *et al.* 2003; Holzner *et al.* 2005c; Walker 2008; Saenger *et al.* 2009b; Lambert *et al.* 2009a).

## PARTICLE MOTION

Assuming that the particle motion of double-frequency microseisms and microtremors (which are mainly composed of Rayleigh waves) are elliptical and that the medium is azimuthally isotropic, then the wave should have a rotational motion in a vertical plane oriented in the azimuthal direction (i.e., in the direction of wave propagation) (Barstow *et al.* 1989; Bromirski and Duennebieer 2002; Tanimoto, Ishimaru and Alvizuri 2006; Bonnefoy-Claudet *et al.* 2006b). If, for example, the wave is actually a Love wave then the motion will be transverse to this. To test this proposition, processing of the data in this study was initially band-pass filtered into a selected frequency window. An azimuth of approach was assumed and the horizontal signals were rotated into a radial component in the assumed direction of approach and the transverse component at 90° to this azimuth. The root-mean-square (rms) of each of the radial and transverse components were calculated. Finally the ratio of the radial energy and transverse energy were computed. This process was repeated for all azimuths from zero to 180°.

In Fig. 12 the ratio between maximum and minimum energy levels of horizontal components for a one hour interval (18:00–19:00 local time for the days 3 and 5 to 8 June) are presented. The time period reflects the days immediately prior to Cyclone Gonu striking the coast of Oman up until it dispersed two days later. For the frequency band 0.25 Hz (double-frequency microseism) a clear correlation exists between the azimuth of maximum energy and the movement of the cyclone along the Omani coast. Before the cyclone had approached the coast, the particle motion tends to be more focused with an azimuth of approach pointing around N98°E (i.e., south-east towards the Arabian Sea). As the cyclone

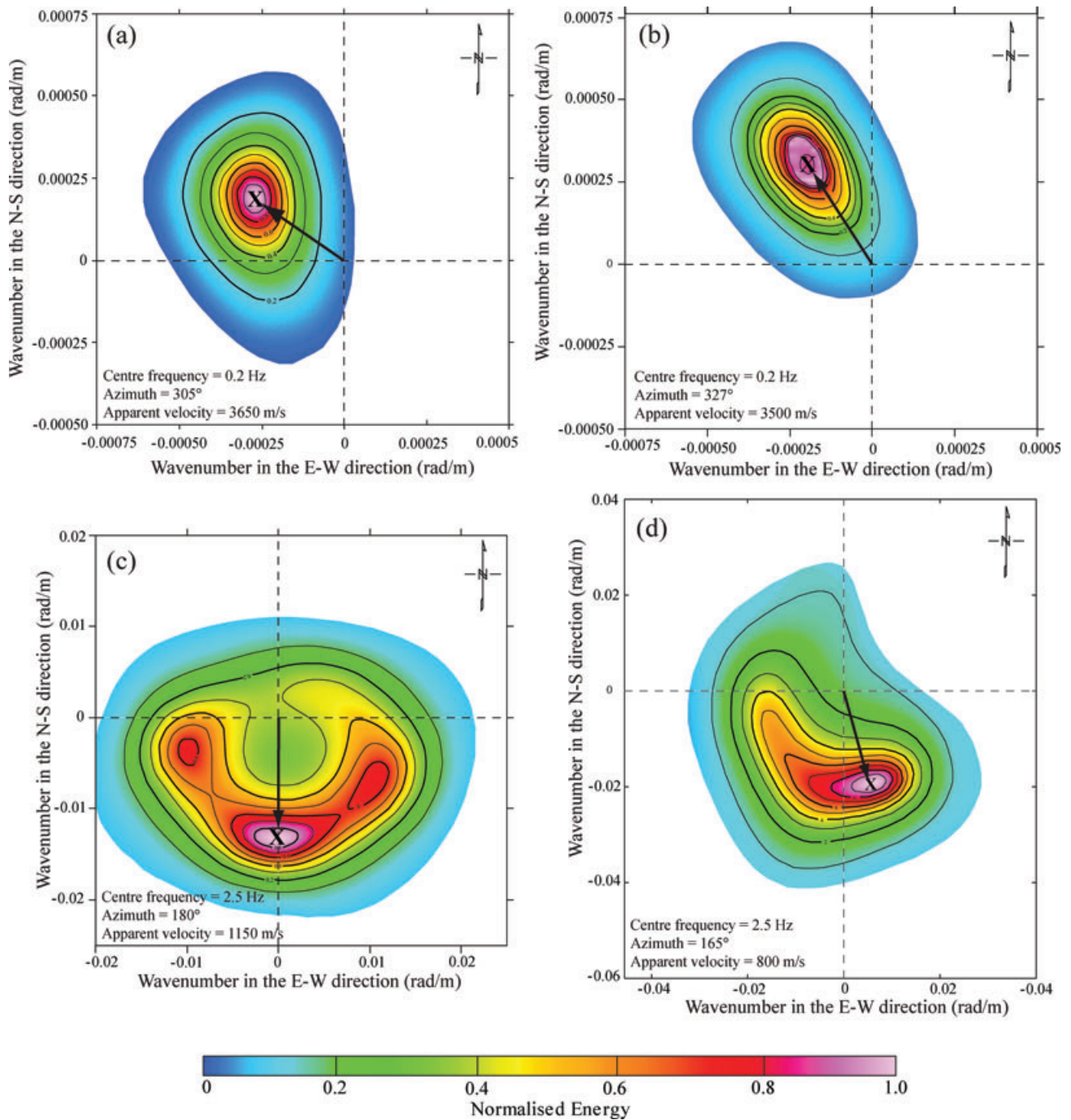


**Figure 11** Normalized energy response in slowness space for arrays of varying aperture sizes at a) location A, oilfield: centre frequency = 0.2 Hz, array aperture = 3600 m, 4 June 2007 at 00:00–01:00. b) Location B, oilfield: centre frequency = 0.2 Hz, array aperture = 3600 m, 16 June 2007 at 00:00–01:00. c) Location A, oilfield: centre frequency = 2.5 Hz with array radius of 225 m, 26 May 2007 at 00:00–01:00. d) Dry well: centre frequency = 2.5 Hz with array radius of 100 m, 20 January 2009 at 00:00–01:00. For locations of the sensors see Fig. 1. In each figure the symbol 'X' indicates the peak values. The distance between the centres and 'X' gives the slowness of the waves at the frequency and the line at the centre to 'X' gives the direction of the wave propagation. The phase velocity and propagation azimuth (from the source) determined from the maximum peak are written in the lower left-hand corner in each plot.

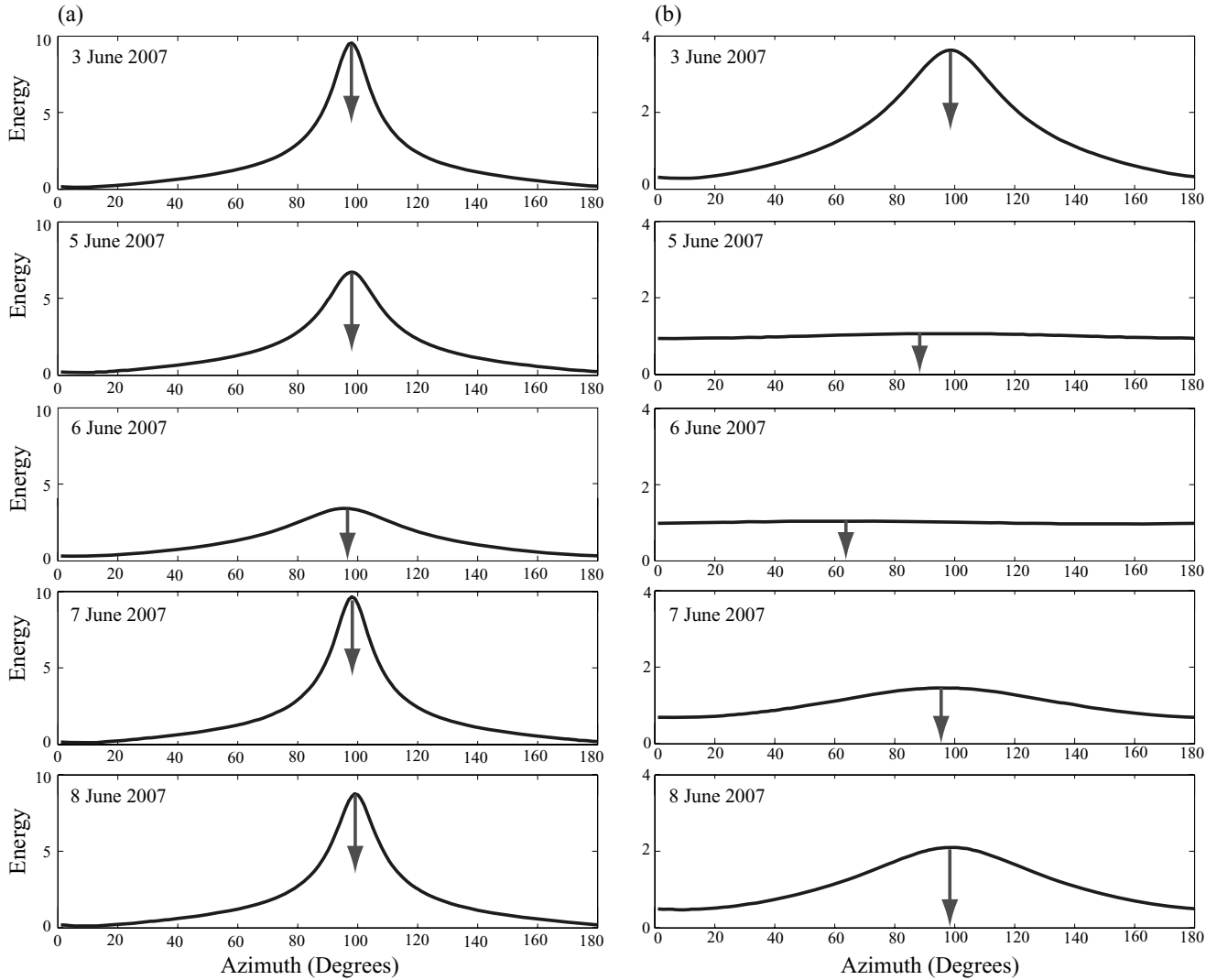


Figure 12 Ratio between maximum and minimum energy of the horizontal components plotted as a function of azimuth a) for microtremor, centre frequency 2.5 Hz and b) for microseism, centre frequency 0.25 Hz. The arrow points the azimuth for maximum energy.

approaches the coast the azimuth shifts towards the east and north-east, whilst becoming less coherent. This effect could be expected as the storm gets nearer to the coast and produces a wider distribution of sources. After the cyclone finally dissipates the azimuth of maximum energy returns to the previous direction.

For the duration of the cyclone, the microtremor signals exhibit minimal notable changes. A de-focusing of the amplitudes can be observed on 6 June but there is no visible change to the peak azimuth. These results are consistent with the results obtained from the frequency-wavenumber analysis and would indicate an independence of sources for the microtremors and microseism signals.

## DISCUSSION

The characteristics of ambient noise recorded over an oilfield and an abandoned exploration well have been investigated in relation to recent claims that signals in the microtremor range can be applied to hydrocarbon detection. The analyses of the data provide a better understanding of the nature and origin of anomalously high microtremor signals that have reportedly been observed over several hydrocarbon reservoirs in the region. The results for this study indicate that high levels of microtremor signals are present above the hydrocarbon reservoir as previously claimed but that similar levels of this signal are also observed over nearby assumed

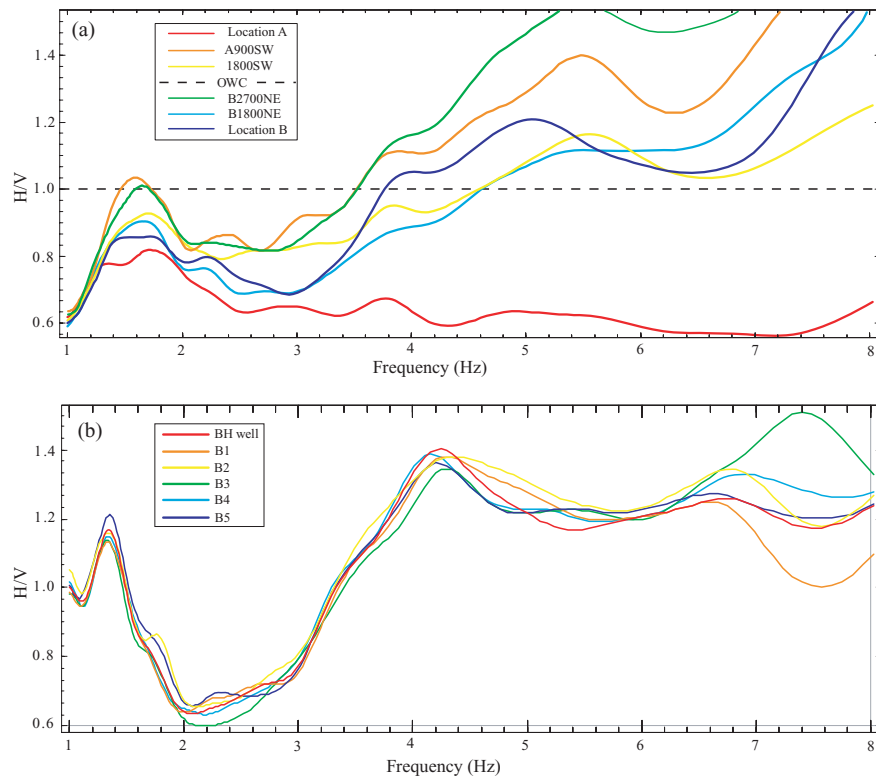


**Figure 13** a) Mean H/V spectral ratio of 60 minutes microtremor data recorded at the oilfield on 7 June 2007 at 00:00–01:00. b) H/V spectral ratio of 60 minutes microtremor data recorded at the dry well on 20 January 2009 at 00:00–01:00.

non-reservoir locations. Moreover, the results indicate that the observed anomalous microtremor signals have originated from surface waves with a propagation back azimuth pointing towards the nearest motorways in the area. Similar findings have been published from other studies. For example, Hanssen and Bussat (2008) examined the relative traveltimes of microtremor measurements over an oilfield in Libya and concluded that the observed waveforms were actually surface waves caused by anthropogenic sources such as production facilities, traffic and the resonance frequencies of unconsolidated overburden in the area.

Whilst it could be suggested that had weak microtremor signals from hydrocarbon reservoirs been present in the survey locations then they may have been masked by the strong anthropogenic noise (e.g., from traffic) and thus not been detected at all without the application of an appropriate filter such as a  $f$ - $k$  filter (Nguyen *et al.* 2009). However, one of the key design criteria in the planning of this survey was to utilize 3-component sensors in graduated arrays that would enable full discrimination of laterally propagating waves from vertical, and to provide detailed information on the phase velocity and direction of approach of any coherent wave energy. This

methodology is in direct contrast to previous surveys which typically relied on simple lines of discrete sensors, thus making it impossible to differentiate individual wave trains based on their propagation characteristics other than frequency content. As demonstrated in this study the best approach to discriminating waveforms originating from multiple sources is to acquire data in arrays. Also, to minimize the effects of anthropogenic noise in this survey, whenever possible data for analysis was specifically selected from the 24 hour records when noise levels were at their lowest (i.e., during the night and early morning).

Although our results clearly indicate that microtremor analysis cannot be used as a hydrocarbon indicator for this area, the data do however have the potential to significantly contribute towards geotechnical characterization of shallow sediments for seismic hazard assessment. For example, it is well documented in the literature (Nakamura 1989; Bodin and Horton 1999; Cara, Di Giulio and Rovelli 2003; Guillier *et al.* 2005; Stephenson *et al.* 2009) that unconsolidated shallow sedimentary layers cause amplification of ambient noise at distinct frequencies in the range of 1–10 Hz, which are related to the geometry and the seismic properties of the soil

layer. As a result microtremor data can be used to estimate fundamental resonant frequencies as well as shear-wave velocities and thickness of the uppermost soft layers.

Figure 13 shows the H/V (reciprocal of V/H) spectral ratio of microtremor measurements of the two survey areas. The fundamental resonance frequency of the oilfield peaks at about 1.7 Hz, with greater variability in terms of H/V envelope. The dry exploration well shows two well-pronounced peaks at 1.3 Hz and 4.2 Hz. The peak at 1.3 Hz most likely represents the fundamental resonance frequencies of the site, whereas the peak at 4.2 Hz may be related to a contrast at deeper depth or industrial origin.

Using the observed fundamental resonance frequencies we calculated the thickness of the soft soil in both survey areas and then compared that result with the well data, according to the well-known equation (Parolai, Bormann and Milkereit 2002)

$$f_{H/V} \approx f_0 = \frac{V_{s,average}}{4h} \quad (2)$$

where  $V_{s,average}$  and  $h$  are the average shear-wave velocity and the thickness of sediments respectively. The shear-wave velocities were estimated to be 815–1220 m/s from array analysis using a high-resolution frequency-wavenumber ( $f$ - $k$ ) spectral technique and from sonic log data from the well.

By use of this argument, the thickness of unconsolidated sediments for the oilfield in this study was estimated to be around 120–180 m. This is consistent with the drilling data close to location A, which penetrated 130 m of Quaternary age aeolian sediments. The thickness of the unconsolidated sediments at the dry exploration well was estimated to be 154 m but this could not be confirmed as the well did not record any data at shallow levels.

This study does not conclusively disprove the assertion that the interaction of microseism energy with porous multi-phase hydrocarbon reservoirs can generate microtremor signals as reported by Dangel (2003), Lambert (2009a) and Saenger (2009b). However, for the sites investigated and described in this paper any signals possibly originating from such interactions have been completely overshadowed by other effects, primarily noise caused by cultural activity. These constraints plus the complete lack of evidence in favour of the microtremor detection technique make such analyses unsuitable for hydrocarbon detection in the environment for this study.

## CONCLUSIONS

The following conclusions are drawn from this study:

- Double-frequency microseism signals are observable within the frequency band of 0.15–0.4 Hz. The spectral amplitudes

of the microseism increased as Cyclone Gonu approached the coast of Oman then declined once the cyclone passed the region. There is no apparent correlation between the microtremor and microseism signals and therefore, the driving force of the microtremor signal cannot be the microseism events.

- Microtremor (2.5–3 Hz) signals are observed over two sites (over an oilfield and above a dry well). During the day all sensors recorded strong microtremor signal, whereas all sensors detected only weak signals over night. There is no direct correlation between the maximum spectral amplitude of microtremors and meteorological data. Cyclical daily and weekly variations in the microtremor spectral amplitudes clearly correlate with human activity.
- V/H spectral ratios of 2.5–3 Hz are observed on both sites. The V/H peak is not related to the location of the known hydrocarbon reservoir.
- Analyses of regional earthquake data show no evidence of earthquake triggered spectral amplitude modification by the hydrocarbon reservoir.
- Particle motion studies clearly show that the microseism signal was influenced by the action of Cyclone Gonu, while the microtremor band displayed no such correlation.
- The apparent velocity and propagation azimuth (from the source) of microseism signals were 3500–3650 m/s and 305–327°, respectively for the oilfield. These results suggest that the source of the microseism is the ocean swells of the Arabian Sea.
- The apparent velocity and propagation azimuth for the microtremor signal recorded at the oilfield and dry well are 800–1150 m/s and 165–180°, respectively. These results indicate that the observed microtremor signals originate from surface waves propagating through shallow sediments having an azimuth directed from the nearest motorways.

## ACKNOWLEDGEMENTS

We are grateful to the Oil Subcommittee of the Abu Dhabi National Oil Co. (ADNOC) and its operating companies (Op-Cos) for sponsoring this project. We thank Mr Marwan Haggag for his logistical support of the fieldwork and in coordinating the project and Islam Md. Didarul for providing the meteorological data.

## REFERENCES

- Ali M.Y., Berteussen K.A., Small J., Anjana B.T. and Barkat B. 2009a. Recent passive experiments in Abu Dhabi. EAGE Passive Seismic Workshop – Exploration and Monitoring Applications, Limassol, Cyprus, Expanded Abstracts, A36.

- Ali M.Y., Berteussen K.A., Small J., Anjana B.T., Barkat B. and Pahlevi O. 2009b. Recent low frequency passive seismic experiments in Abu Dhabi. 71<sup>st</sup> EAGE meeting, Amsterdam, The Netherlands, Expanded Abstracts, S037.
- Ali M.Y., Berteussen K.A., Small J. and Barkat B. 2007. A low frequency passive seismic experiment over a carbonate reservoir in Abu Dhabi. *First Break* 25, 71–73.
- Ali M.Y., Berteussen K.A., Small J., Barkat B. and Pahlevi O. 2009c. Results from a low frequency passive seismic experiment over an oilfield in Abu Dhabi. *First Break* 27, 91–97.
- Ali M.Y., Berteussen K.A., Small J. and Pahlevi O. 2009d. Microseism and microtremor analyses over an oilfield in Abu Dhabi – Implications for cyclone and hydrocarbon detection. 71<sup>st</sup> EAGE meeting, Amsterdam, The Netherlands, Expanded Abstracts, SO34.
- Ali M.Y. and Watts A.B. 2009. Subsidence history, gravity anomalies and flexure of the United Arab Emirates (UAE) foreland basin. *Georabia* 14, 17–44.
- Ansal A.M., Iyisan R. and Gullu H. 2001. Microtremor measurements for the microzonation of Dinar. *Pure and Applied Geophysics* 158, 2525–2541.
- Barstow N., Sutton G.H. and Carter J.A. 1989. Particle motion and pressure relationships of ocean bottom noise at 3900 m depth: 0.003 to 5 Hz. *Geophysical Research Letters* 16, 1185–1188.
- Berteussen K.A., Ali M.Y., Small J., Anjana B.T. and Barkat B. 2008a. Analysis of low frequency passive seismic data from an experiment over a carbonate reservoir in Abu Dhabi. Abu Dhabi International Petroleum Exhibition and Conference, Abu Dhabi, United Arab Emirates, SPE -117925-MS.
- Berteussen K.A., Ali M.Y., Small J. and Barkat B. 2008b. A low frequency, passive seismic experiment over a carbonate reservoir in Abu Dhabi – Wavefront and particle motion study. 70<sup>th</sup> EAGE meeting, Rome, Italy, Expanded Abstracts, B046.
- Bhattarai M. 2005. Seismic microzonation using H/V spectral ratios with single station microtremor survey. *Individual Studies by Participants at the International Institute of Seismology and Earthquake Engineering* 41, 73–86.
- Bloch G. and Akrawi K. 2006. Application of passive seismic (IPDS) surveys in Arabian Peninsula. EAGE passive seismic workshop – Exploration and monitoring applications, Dubai, United Arab Emirates, Expanded Abstracts, A28.
- Bodin P. and Horton S. 1999. Broadband microtremor observation of basis resonance in the Mississippi embayment, Central US. *Geophysical Research Letters* 26, 903–906.
- Bonnefoy-Claudet S., Cornou C., Bard P.Y., Cotton F., Moczo P., Kristek J. and Fah D. 2006a. H/V ratio: a tool for site effects evaluation. Results from 1-D noise simulations. *Geophysical Journal International* 167, 827–837.
- Bonnefoy-Claudet S., Cotton F. and Bard P.Y. 2006b. The nature of noise wavefield and its applications for site effects studies – A literature review. *Earth-Science Reviews* 79, 205–227.
- Bromirski P.D. and Duennebieer F.K. 2002. The near-coastal microseism spectrum: Spatial and temporal wave climate relationships. *Journal of Geophysical Research-Solid Earth* 107, 2166. doi:10.1029/2001JB000265
- Bromirski P.D., Duennebieer F.K. and Stephen R.A. 2005. Mid-ocean microseisms. *Geochemistry Geophysics Geosystems* 6, Q04009. doi:10.1029/2004GC000768.
- Capon J. 1969. High-resolution frequency-wavenumber spectrum analysis. *Proceedings of the IEEE* 57, 1408–1418.
- Cara F., Cultrera G., Azzara R.M., De Rubeis V., Di Giulio G., Giammarinaro M.S. et al. 2008. Microtremor measurements in the city of Palermo, Italy: Analysis of the correlation between local geology and damage. *Bulletin of the Seismological Society of America* 98, 1354–1372.
- Cara F., Di Giulio G. and Rovelli A. 2003. A study on seismic noise variations at Colfiorito, central Italy; Implications for the use of H/V spectral ratios. *Geophysical Research Letters* 30, 1972. doi:10.1029/2003GL017807.
- Cessaro R.K. 1994. Sources of primary and secondary microseisms. *Bulletin of the Seismological Society of America* 84, 142–148.
- Chavez-Garcia F.J. and Luzon F. 2005. On the correlation of seismic microtremors. *Journal of Geophysical Research-Solid Earth* 110, B08302.
- Chavez-Garcia F.J. and Rodriguez M. 2007. The correlation of microtremors: empirical limits and relations between results in frequency and time domains. *Geophysical Journal International* 171, 657–664.
- Chevrot S., Sylvander M., Benahmed S., Ponsolles C., Lefevre J.M. and Paradis D. 2007. Source locations of secondary microseisms in western Europe: Evidence for both coastal and pelagic sources. *Journal of Geophysical Research-Solid Earth* 112, B11301. doi:10.1029/2007JB005059
- Cho I., Tada T. and Shinozaki Y. 2006. A generic formulation for microtremor exploration methods using three-component records from a circular array. *Geophysical Journal International* 165, 236–258.
- Cohen L. 1995. *Time-Frequency Analysis*. Prentice-Hall.
- le Comte D. 2008. Global Weather Highlights 2007: A mixed bag. *Weatherwise* 61, 16–18.
- Dangel S., Schaepman M.E., Stoll E.P., Carniel R., Barzandji O., Rode E.D. and Singer J.M. 2003. Phenomenology of tremor-like signals observed over hydrocarbon reservoirs. *Journal of Volcanology and Geothermal Research* 128, 135–158.
- De Bhowmick A.K., Thani M.A. and Al-Rawahi Y. 2007. Cyclone ‘GONU’ and reliability of main interconnected transmission system of Oman. IEEE Conference, Perth, Australia, Expanded Abstracts, 48–52.
- Di Giulio G., Cornou C., Ohrnberger M., Wathélet M. and Rovelli A. 2006. Deriving wavefield characteristics and shear-velocity profiles from two-dimensional small-aperture arrays analysis of ambient vibrations in a small-size alluvial basin, Colfiorito, Italy. *Bulletin of the Seismological Society of America* 96, 1915–1933.
- Draganov D., Campman X., Thorbecke J., Verdel A. and Wapenaar K. 2009. Subsurface structure from ambient seismic noise. 71<sup>st</sup> EAGE meeting, Amsterdam, The Netherlands, Expanded Abstracts, Z038.
- Draganov D., Wapenaar K., Mulder W., Singer J. and Verdel A. 2007. Retrieval of reflections from background-noise measurements. *Geophysical Research Letters* 34, L04305.
- Dutta U., Satoh T., Kawase H., Sato T., Biswas N., Martirosyan A. and Dravinski M. 2007. S-wave velocity structure of sediments in Anchorage, Alaska, estimated with array measurements of microtremors. *Bulletin of the Seismological Society of America* 97, 234–255.

- Frehner M., Schmalholz S.M., Holzner R. and Podladchikov Y.Y. 2006. Interpretation of hydrocarbon microtremors as pore fluid oscillations driven by ambient seismic noise. EAGE Passive Seismic Workshop – Exploration and Monitoring Applications, Dubai, United Arab Emirates, Expanded Abstracts, A05.
- Frehner M., Schmalholz S.M. and Podladchikov Y. 2009. Spectral modification of seismic waves propagating through solids exhibiting a resonance frequency: A 1-D coupled wave propagation-oscillation model. *Geophysical Journal International* 176, 589–600.
- Frehner M., Schmalholz S.M., Podladchikov Y., Eth Z. and Oslo U. 2007. Interaction of seismic background noise with oscillating pore fluids causes spectral modifications of passive seismic measurements at low frequencies. 77<sup>th</sup> SEG meeting, San Antonio, Texas, USA, 1307–1311.
- Friedrich A., Krüger F. and Klinge K. 1998. Ocean-generated microseismic noise located with the Gräfenberg array. *Journal of Seismology* 2, 47–64.
- Gaull B.A., Kagami H. and Taniguchi H. 1995. The microzonation of Perth, Western Australia, using microtremor spectral ratios. *Earthquake Spectra* 11, 173–191.
- Gerstoft P., Fehler M.C. and Sabra K.G. 2006. When Katrina hit California. *Geophysical Research Letters* 33, L17308. doi:10.1029/2006GL027270
- Goertz A.V., Schechinger B., Koerbe M. and Krajewski P. 2009. A low-frequency passive seismic survey in an urban setting in Germany. 71<sup>st</sup> EAGE meeting, Amsterdam, The Netherlands, Expanded Abstracts, S039.
- Graf R., Schmalholz S.M., Podladchikov Y.Y. and Saenger E.H. 2007. Passive low frequency spectral analysis: Exploring a new field in geophysics. *World Oil* 228, 47–52.
- Green A. and Greenhalgh S. 2009. Microtremor spectra: A proven means for estimating resonant frequencies and S-wave velocities of shallow soils/sediments, but a questionable tool for locating hydrocarbon reservoirs. *First Break* 27, 5–11.
- Grevemeyer I., Herber R. and Essen H.H. 2000. Microseismological evidence for a changing wave climate in the northeast Atlantic Ocean. *Nature* 408, 349–352.
- Guillier B., Chatelain J.L., Hellel M., Machane D., Mezouer N., Ben Salem R. and Oubaiche E.H. 2005. Smooth bumps in H/V curves over a broad area from single-station ambient noise recordings are meaningful and reveal the importance of Q in array processing: The Boumerdes (Algeria) case. *Geophysical Research Letters* 32, L24306. doi:10.1029/2005GL023726
- Haghshenas E., Bard P.Y., Theodulidis N. and the SESAME WP04 Team. 2008. Empirical evaluation of microtremor H/V spectral ratio. *Bulletin of Earthquake Engineering* 6, 75–108.
- Hanssen P. and Bussat S. 2008. Pitfalls in the analysis of low frequency passive seismic data. *First Break* 26, 111–119.
- Hartzell S., Carver D., Williams R.A., Harmsen S. and Zerva A. 2003. Site response, shallow shear-wave velocity and wave propagation at the San Jose, California, dense seismic array. *Bulletin of the Seismological Society of America* 93, 443–464.
- Haubrich R.A. and McCamy K. 1969. Microseisms; Coastal and pelagic sources. *Reviews of Geophysics* 7, 539–571.
- Holzner R., Eschle P., Dangel S., Frehner M., Narayanan C. and Lakehal D. 2009. Hydrocarbon microtremors interpreted as nonlinear oscillations driven by oceanic background waves. *Communications in Nonlinear Science & Numerical Simulation* 14, 160–173.
- Holzner R., Eschle P., Dangel S. and Narayanan C. 2007a. Hydrocarbon related microtremors – Verification of an analytical oscillator model by the Navier-Stokes equations. 69<sup>th</sup> EAGE meeting, London, UK, Expanded Abstracts, P212.
- Holzner R., Eschle P., Dewarrat R., Lambert M. and Graf R. 2006c. Marine application of hydrocarbon microtremor analysis (HyMAS). 76<sup>th</sup> SEG meeting, New Orleans, Louisiana, USA, 2290–2293.
- Holzner R., Eschle P., Frehner M., Schmalholz S. and Podladchikov Y. 2006a. Hydrocarbon microtremors interpreted as oscillations driven by oceanic background waves. 68<sup>th</sup> EAGE meeting, Vienna, Austria, Expanded Abstracts, D036.
- Holzner R., Eschle P., Frehner M., Schmalholz S. and Podladchikov Y. 2006b. Interpretation of hydrocarbon microtremors as nonlinear oscillations driven by oceanic background waves. 76<sup>th</sup> SEG meeting, New Orleans, Louisiana, USA, 2294–2298.
- Holzner R., Eschle P., Meier P.F. and Dangel S. 2007b. Linear model for low-frequency pore liquid oscillations observed in hydrocarbon microtremor analysis (HyMAS). *GeoArabia* 12, 169.
- Holzner R., Eschle P., Zurcher H., Graf R., Dangel S. and Meier P.F. 2005a. Identification of hydrocarbon reservoirs by microtremor analysis (HyMAS) – Successful and reproducible. 2<sup>nd</sup> SEG/EGS/EPEX/EPA International Petroleum Conference, Cairo, Egypt, 36.
- Holzner R., Eschle P., Zurcher H., Graf R., Dangel S. and Meier P.F. 2005b. Case study of successful identification of hydrocarbon reservoirs by microtremor analysis (HyMAS). AAPG International Conference, Paris, France.
- Holzner R., Eschle P., Zurcher H., Lambert M., Graf R., Dangel S. and Meier P.F. 2005c. Applying microtremor analysis to identify hydrocarbon reservoirs. *First Break* 23, 41–46.
- Horike M., Zhao B. and Kawase H. 2001. Comparison of site response characteristics inferred from microtremors and earthquake shear waves. *Bulletin of the Seismological Society of America* 91, 1526–1536.
- Kedar S. and Webb F.H. 2005. The ocean's seismic hum. *Science* 307, 682–683.
- Kind F., Faeh D. and Giardini D. 2005. Array measurements of S-wave velocities from ambient vibrations. *Geophysical Journal International* 160, 114–126.
- Konno K. and Ohmachi T. 1998. Ground-motion characteristics estimated from spectral ratio between horizontal and vertical components of microtremor. *Bulletin of the Seismological Society of America* 88, 228–241.
- Lambert M., Schmalholz S.M., Saenger E.H. and Podladchikov Y.Y. 2007. Low-frequency anomalies in spectral ratios of single-station microtremor measurements: Observations across an oil and gas field in Austria. 77<sup>th</sup> SEG meeting, San Antonio, Texas, USA, Expanded Abstracts, 1352–1356.
- Lambert M.-A., Schmalholz S.M., Saenger E.H. and Steiner B. 2009a. Low-frequency microtremor anomalies at an oil and gas field in Voitsdorf, Austria. *Geophysical Prospecting* 57, 393–411. doi:10.1111/j.1365-2478.2008.00734.x
- Lambert M.A., Schmalholz S.M., Saenger E.H. and Steiner B. 2009b. Passive seismic study at an oil and gas field in Voitsdorf, Austria.

- EAGE Passive Seismic Workshop – Exploration and Monitoring Applications, Limassol, Cyprus, Expanded Abstracts, A34.
- Lermo J. and Chavez-Garcia F.J. 1994. Are microtremors useful in site response evaluation? *Bulletin of the Seismological Society of America* **84**, 1350–1364.
- Liu H.-P., Boore D.M., Joyner W.B., Oppenheimer D.H., Warrick R.E., Zhang W. *et al.* 2000. Comparison of phase velocities from array measurements of Rayleigh waves Associated with microtremor and results calculated from borehole shear-wave velocity profiles. *Bulletin of the Seismological Society of America* **90**, 666–678.
- Longuet-Higgins M.S. 1950. A theory of the origin of microseisms. *Philosophical Transactions of the Royal Society of London A* **243**, 1–35.
- Louie J.N. 2001. Faster, better: Shear-wave velocity to 100 meters depth from refraction microtremor arrays. *Bulletin of the Seismological Society of America* **91**, 347–364.
- Maresca R., Galluzzo D. and Del Pezzo E. 2006. H/V spectral ratios and array techniques applied to ambient noise recorded in the Colfiorito Basin, central Italy. *Bulletin of the Seismological Society of America* **96**, 490–505.
- Marzorati S. and Bindi D. 2006. Ambient noise levels in north central Italy. *Geochemistry Geophysics Geosystems* **7**, Q09010, doi:10.1029/2006GC001256.
- van Mastrigt P. and Al-Dulaijan A. 2008. Seismic spectroscopy using amplified 3C geophones. 70th EAGE meeting, Rome, Italy, Expanded Abstracts, B047.
- McNamara D.E. and Buland R.P. 2004. Ambient noise levels in the continental United States. *Bulletin of the Seismological Society of America* **94**, 1517–1527.
- Nakamura Y. 1989. A method for dynamic characteristics estimation of subsurface using microtremor on the ground surface. *Quarterly Report Railway Technical Research Institute* **30**, 25–30.
- Nguyen T.T., Lambert M., Saenger E.H., Artman B. and Schmalholz S.M. 2009. Reduction of noise effects on low frequency passive seismic data. 71<sup>st</sup> EAGE meeting, Amsterdam, the Netherlands, Expanded Abstracts, S038.
- Nguyen T.T., Saenger E.H., Schmalholz S.M. and Artman B. 2008. Earthquake triggered modifications of microtremor signals above and nearby a hydrocarbon reservoir in Voitsdorf, Austria. 70<sup>th</sup> EAGE meeting, Rome, Italy, Expanded Abstracts, P025.
- Ohoiri M., Nobata A. and Wakamatsu K. 2002. A Comparison of ESAC and FK methods of estimating phase velocity using arbitrarily shaped microtremor arrays. *Bulletin of the Seismological Society of America* **92**, 2323–2332.
- Okada H. 2003. *The Microtremor Survey Method*. Geophysica. SEG. ISBN 1560801204.
- Parolai S., Bormann P. and Milkereit C. 2002. New relationships between  $V_s$ , thickness of sediments, and resonance frequency calculated by the H/V ratio of seismic noise for the Cologne area (Germany). *Bulletin of the Seismological Society of America* **92**, 2521–2527.
- Peterson J. 1993. Observations and modeling of seismic background noise. US Geological Survey, Open File Report, 93–322, 1–95.
- Picozzi M., Parolai S. and Richwalski S.M. 2005. Joint inversion of H/V ratios and dispersion curves from seismic noise: Estimating the S-wave velocity of bedrock. *Geophysical Research Letters* **32**, L11308, doi:10.1029/2005GL022878.
- Rached G.R. 2006. Surface passive seismic in Kuwait. EAGE Passive Seismic Workshop – Exploration and Monitoring Applications, Dubai, United Arab Emirates, Expanded Abstracts, A27.
- Rached G.R. 2009. The challenge for surface passive seismic measurements in Kuwait. EAGE Passive Seismic Workshop – Exploration and Monitoring Applications, Limassol, Cyprus, Expanded Abstracts, A33.
- Rodriguez V.H.S. and Midorikawa S. 2003. Comparison of spectral ratio techniques for estimation of site effects using microtremor data and earthquake motions recorded at the surface and in boreholes. *Earthquake Engineering & Structural Dynamics* **32**, 1691–1714.
- Saenger E.H., Lambert M.A., Nguyen T.T. and Schmalholz S.M. 2009a. Preliminary model of hydrocarbon reservoir related microtremors. 71<sup>st</sup> EAGE meeting, Amsterdam, the Netherlands, Expanded Abstracts, S035.
- Saenger E.H., Schmalholz S.M., Lambert M.A., Nguyen T.T., Torres A., Metzger S. *et al.* 2009b. A passive seismic survey over a gas field: Analysis of low-frequency anomalies. *Geophysics* **74**, O29–O40.
- Saenger E.H., Schmalholz S.M., Podladchikov Y.Y., Holzner R., Lambert M., Steiner B. *et al.* 2007a. Scientific strategy to explain observed spectral anomalies over hydrocarbon reservoirs generated by microtremors. 69<sup>th</sup> EAGE meeting, London, UK, Expanded Abstracts, A033.
- Saenger E.H., Torres A. and Artman B. 2009c. A low-frequency passive seismic survey in Libya. EAGE Detective Stories Behind Prospect Generation Workshop – Challenges and The Way Forward, Muscat, Oman, Expanded Abstracts, 5028.
- Saenger E.H., Torres A., Rentsch S., Lambert M., Schmalholz S.M. and Mendez H.E. 2007b. A hydrocarbon microtremor survey over a gas field: Identification of seismic attributes. 77<sup>th</sup> SEG meeting, San Antonio, Texas, USA, Expanded Abstracts, 1277–1281.
- Satoh T., Kawase H. and Matsushima S. 2001. Estimation of S-wave velocity structures in and around the Sendai basin, Japan, using array records of microtremors. *Bulletin of the Seismological Society of America* **91**, 206–218.
- Scherbaum F., Hinzen K.G. and Ohrnberger M. 2003. Determination of shallow shear wave velocity profiles in the Cologne, Germany area using ambient vibrations. *Geophysical Journal International* **152**, 597–612.
- Schmalholz S.M., Podladchikov Y.Y., Holzner R. and Saenger E.H. 2006. Scientific strategy to explain observed spectral anomalies over hydrocarbon reservoirs generated by microtremors. EAGE Passive Seismic Workshop – Exploration and Monitoring Applications, Dubai, United Arab Emirates, Expanded Abstracts, A06.
- Singer J.M., Barzandji O., Leu W., Rode E.D., Akrawi K., Linthorst S. and Dangel S. 2002. Spectroscopic identification of tremor phenomena over hydrocarbon reservoirs. 64<sup>th</sup> EAGE meeting, Florence, Italy, Expanded Abstracts, H-46.
- Steiner B., Saenger E.H. and Schmalholz S.M. 2007. Time-reverse modeling of microtremors: A potential method for hydrocarbon reservoir localization. 77<sup>th</sup> SEG meeting, San Antonio, Texas, USA, Expanded Abstracts, 2115–2119.
- Steiner B., Saenger E.H. and Schmalholz S.M. 2008a. Case studies on 2D- and 3D-time reverse modeling of low-frequency microtremors

- Application to reservoir localization. 70<sup>th</sup> EAGE meeting, Rome, Italy, Expanded Abstracts, B045.
- Steiner B., Saenger E.H. and Schmalholz S.M. 2008b. Time reverse modeling of low-frequency microtremors: Application to hydrocarbon reservoir localization. *Geophysical Research Letters* **35**, L03307. doi:10.1029/2007GL032097
- Stephenson W.J., Hartzell S., Frankel A.D., Asten M., Carver D.L. and Kim W.Y. 2009. Site characterization for urban seismic hazards in lower Manhattan, New York City, from microtremor array analysis. *Geophysical Research Letters* **36**, L03301, doi:10.1029/2008GL036444
- Tada T., Cho I. and Shinozaki Y. 2006. A two-radius circular array method; inferring phase velocities of Love waves using microtremor records. *Geophysical Research Letters* **33**, L10303, doi:10.1029/2006GL025722
- Tada T., Cho I. and Shinozaki Y. 2007. Beyond the SPAC method: Exploiting the wealth of circular-array methods for microtremor exploration. *Bulletin of the Seismological Society of America* **97**, 2080–2095.
- Tanimoto T. 2007. Excitation of normal modes by non-linear interaction of ocean waves. *Geophysical Journal International* **168**, 571–582.
- Tanimoto T., Ishimaru S. and Alvizuri C. 2006. Seasonality in particle motion of microseisms. *Geophysical Journal International* **166**, 253–266.
- Tuladhar R., Yamazaki F., Warnitchai P. and Saita J. 2004. Seismic microzonation of the greater Bangkok area using microtremor observations. *Earthquake Engineering & Structural Dynamics* **33**, 211–225.
- Walker D. 2008. Recent developments in low frequency spectral analysis of passive seismic data. *First Break* **26**, 69–77.
- Wathelet M., Jongmans D., Ohrnberger M. and Bonnefoy-Claudet S. 2008. Array performances for ambient vibrations on a shallow structure and consequences over Vs inversion. *Journal of Seismology* **12**, 1–19.
- Webb S.C. 2007. The Earth's 'hum' is driven by ocean waves over the continental shelves. *Nature* **445**, 754–756.
- Wilson D., Leon J., Aster R., Ni J., Schlue J., Grand S. *et al.* 2002. Broadband seismic background noise at temporary seismic stations observed on a regional scale in the southwestern United States. *Bulletin of the Seismological Society of America* **92**, 3335–3342.
- Withers M.M., Aster R.C., Young C.J. and Chael E.P. 1996. High-frequency analysis of seismic background noise as a function of wind speed and shallow depth. *Bulletin of the Seismological Society of America* **86**, 1507–1515.
- Yamanaka H., Dravinski M. and Kagami H. 1993. Continuous measurements of microtremors on sediments and basement in Los Angeles, California. *Bulletin of the Seismological Society of America* **83**, 1595–1609.
- Young C.J., Chael E.P., Withers M.M. and Aster R.C. 1996. A comparison of the high-frequency (>1Hz) surface and subsurface noise environment at three sites in the United States. *Bulletin of the Seismological Society of America* **86**, 1516–1528.